Gersonde, R., Hodell, D.A., and Blum, P. (Eds.)
Proceedings of the Ocean Drilling Program, Scientific Results Volume 177

Leg 177 Synthesis: Insights into Southern Ocean Paleoceanography on Tectonic to Millennial Timescales[1]

D.A. Hodell,[2] R. Gersonde,[3] and P. Blum[4]

ABSTRACT

Ocean Drilling Program Leg 177 was designed to study the evolution of the South Atlantic sector of the Southern Ocean on tectonic to millennial timescales. Toward this end, we recovered high-quality sedimentary sequences at seven sites between 41° and 53°S, which constitute the raw material for studying the Cenozoic history of the high-latitude South Atlantic Ocean. Here we summarize the principal findings made by shipboard scientists that have been reported in numerous publications since the completion of Leg 177 and provide a historical summary of the development of this sector of the Southern Ocean.

INTRODUCTION

Between 9 December 1997 and 5 February 1998 during Leg 177, seven sites were drilled in the eastern Atlantic sector of the Southern Ocean. This marked the return of the *JOIDES Resolution* to the Southern Ocean after an almost 10-yr hiatus in drilling of the high southern latitudes. We targeted this region because paleoceanographers, paleoclimatologists, and geochemists have become increasingly aware that processes occurring in the Southern Ocean have played a major role in defining the Earth's climate system throughout the Cenozoic. Leg 177 sites are arrayed along a north-south transect from 41° to 53°S (Fig. F1),

F1. Transect of Leg 177 sites, p. 31.

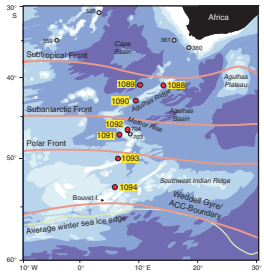

[1]Hodell, D.A., Gersonde, R., and Blum, P., 2002. Leg 177 synthesis: insights into Southern Ocean paleoceanography on tectonic to millennial timescales. *In* Gersonde, R., Hodell, D.A., and Blum, P. (Eds.), *Proc. ODP, Sci. Results,* 177, 1–54 [Online]. Available from World Wide Web: <http://www-odp.tamu. edu/publications/177_SR/VOLUME/SYNTH/SR177SYN.PDF>. [Cited YYYY-MM-DD]
[2]Department of Geological Sciences, University of Florida, 241 Williamson Hall, PO Box 112120, Gainesville FL 32611-2120, USA.
dhodell@geology.ufl.edu
[3]Alfred Wegener Institute for Polar and Marine Research, Columbusstrasse, PO Box 120161, D-27568 Bremerhaven, Germany.
[4]Ocean Drilling Program, Texas A&M University, 1000 Discovery Drive, College Station TX 77845-9547, USA.

Initial receipt: 12 December 2001
Acceptance: 10 September 2002
Web publication: 20 December 2002
Ms 177SR-101

crossing each of the major surface frontal boundaries of the Antarctic Circumpolar Current (ACC). Water depths range from 1974 to 4620 m, intersecting most major subsurface water masses in the South Atlantic (Fig. F2). We succeeded in accomplishing nearly all of our coring objectives, recovering a total of >4000 m of sediment ranging in age from the middle Eocene to Holocene. At most sites, multiple holes were drilled to ensure complete recovery of the stratigraphic section. A complete description of the Leg 177 sediments recovered and shipboard analyses performed is given in the Leg 177 *Initial Reports* volume (Gersonde, Hodell, Blum, et al., 1999). At the time of writing, 4 yr has elapsed since we set sail on Leg 177. Shipboard scientists have had an opportunity to analyze samples in their laboratories, and postcruise scientific results are now being published. Our purpose here is to present an overview of Leg 177 science to date by synthesizing individual reports and evaluating our progress toward meeting the overall leg objectives. We have also included some results obtained on piston cores retrieved by the *Polarstern* and *Thomas G. Thompson* (TTN057) as part of the site survey for Leg 177 because many of these cores have been spliced with the upper sections of Ocean Drilling Program (ODP) cores to obtain complete sections. Most of the Leg 177 papers are contained within this volume or in two special issues of *Marine Micropaleontology* (July 2002, Volume 45, Issues 3–4, pp. 191–402) and *Palaeogeography, Palaeoclimatology, Palaeoecology* (July 2002, Volume 182, Issues 3–4, pp. 145–355) (Gersonde and Hodell, 2002), designed to highlight the biostratigraphic and paleoceanographic results of Leg 177, respectively. Many papers have also been submitted or published in other mainstream journals. The bibliography at the end of this chapter contains a list of Leg 177 papers that was complete at the time of publication and will be updated continually on ODP's web site (**www-odp.tamu.edu/publications/pubs_ct.html**). The CD-ROM included with this booklet contains the Leg 177 papers and data reports submitted to ODP and completed by the time of printing.

F2. Distribution of DIC $\delta^{13}C$, p. 32.

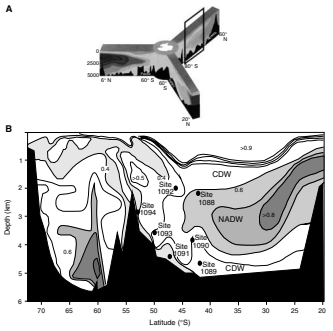

SCIENTIFIC OBJECTIVES AND RESULTS

The ambitious goals of Leg 177 were (1) to document the biostratigraphic, biogeographic, paleoceanographic, and paleoclimatic history of the Southern Ocean during the Cenozoic, including the evolution and stability of the Antarctic cryosphere, and (2) to reconstruct paleoceanographic and paleoclimatic changes in the high-latitude South Atlantic during the Quaternary and late Neogene and determine the role the South Atlantic sector of the Southern Ocean played in global climate change on orbital and suborbital timescales. Full realization of these goals will take years or even decades, but substantial progress has been made toward achieving many of the leg objectives. Essential to all Leg 177 goals is the development of accurate chronologies for each site. First, we review the postcruise results of integrated isotopic, biomagnetic, and geomagnetic stratigraphies. Next, we present the postcruise paleoceanographic findings in chronological order through the Cenozoic.

STRATIGRAPHY

Our purpose here is not to review the details of postcruise stratigraphic studies, but rather to point readers to the literature that has enhanced the wealth of shipboard stratigraphic information contained in the Leg 177 *Initial Reports* volume (Gersonde, Hodell, Blum, et al., 1999).

Biostratigraphy

Studies of diatom biostratigraphy by Censarek and Gersonde (2002) and Zielinski and Gersonde (2002) have enhanced the Miocene and Pliocene–Pleistocene zonation of Leg 177 sites. Both studies revealed latitude-dependent differences in the stratigraphic ranges of diatoms, including key biostratigraphic marker species that are related to development and migration of surface-water masses within the ACC during the Neogene and Pleistocene. New biostratigraphic marker species were defined that assist in the identification of marine isotope Stages (MISs) 6 and 8 in the highest-latitude Leg 177 Sites 1093 and 1094 (Zielinski et al., 2002). Shipboard nannofossil biostratigraphy has been revised for the Pleistocene of all seven Leg 177 sites (Flores and Marino, 2002), the Miocene and Pliocene of Sites 1088 and 1090 (Marino and Flores, **Chap. 7,** this volume), and the middle Eocene to lower Oligocene of Site 1090 (Marino and Flores, **Chap. 8,** this volume). Galeotti et al. (2002) refined the planktonic foraminiferal stratigraphy of the middle Eocene to lower Pliocene section of Site 1090.

Stable Isotope Stratigraphy

While aboard ship, we used variations in sediment physical properties (mainly weight percent carbonate) in conjunction with biomagnetostratigraphy to predict the position of marine isotope stages (see fig. F11 in Shipboard Scientific Party, 1999, p. 45). Hodell et al. (**Chap. 9,** this volume) compiled the oxygen isotope stratigraphies for Sites 1088, 1090, 1090, 1093, and 1094 and compared the results to the shipboard color reflectance data (Figs. **F3, F4**). In all but Site 1089, the shipboard prediction of the position of isotope stages proved to be fairly accurate. Kleiven and Jansen (**Chap. 12,** this volume) developed oxygen isotope stratigraphies for MISs 18 through 26 (early–mid Pleistocene) at Sites 1091 and 1094. Andersson et al. (2002) identified the major oxygen isotope events of the lower and lower upper Pliocene section of Site 1092 (Fig. **F4**). Billups et al. (2002) used the benthic oxygen and carbon isotope record at Site 1090 between ~25 and 16 Ma to correlate to the astronomically tuned isotopic signal at Site 929 on the Ceara Rise (Fig. **F5**) (Shackleton et al., 1999, 2000).

Magnetostratigraphy

Channell and Stoner (2002) refined the polarity reversal stratigraphy of the high-resolution Pliocene–Pleistocene sections of Sites 1089, 1091, 1093, and 1094 by analyzing discrete samples that underwent complete demagnetization. Two studies have augmented the paleomagnetic results obtained onboard ship on the middle Eocene–lower Miocene section at Sites 1090 and the upper Miocene section of Site 1092 by measuring discreet samples and U-channel samples from the composite

F3. Oxygen isotope and color reflectance, p. 33.

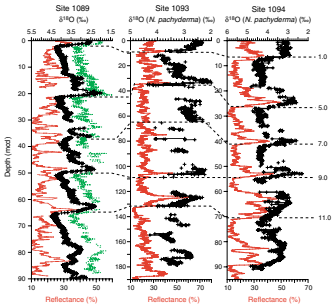

F4. Benthic $\delta^{18}O$ with the reference signal, p. 34.

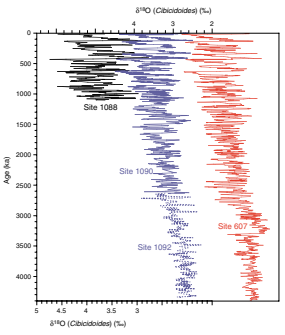

F5. Benthic $\delta^{18}O$ signal vs. Site 929, p. 35.

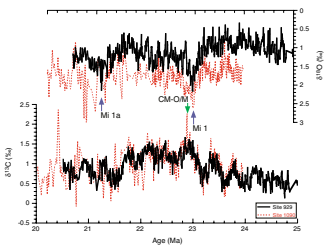

sections (Channell et al., in press; Evans and Channell, in press). In addition to geomagnetic polarity reversals, variations in the paleointensity of the Earth's dipole magnetic field are proving useful for long-distance correlation. Studies of Leg 177 site survey piston cores demonstrated that a paleointensity signal could be extracted from South Atlantic sediments (Fig. F6) (Channell et al., 2000; Stoner et al., 2002). One of the objectives of Leg 177 was to extend these records further back in time. To date, a long paleointensity record has been produced from Site 1089 for the past 450 k.y. (Stoner et al., in press). Although some diagenetic alteration of magnetization intensity has occurred downcore, the relative paleointensity signal from Site 1089 can be correlated to similar high-resolution paleointensity records from the North Atlantic and lower-resolution globally stacked composites (Fig. F7). This study demonstrated that together with traditional oxygen isotope stratigraphy, paleointensity is a powerful new tool for optimizing global stratigraphies.

F6. Geomagnetic paleointensity records, p. 36.

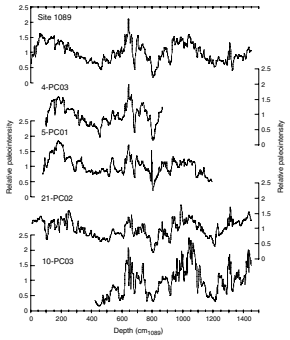

F7. Correlation of oxygen isotope records, p. 37.

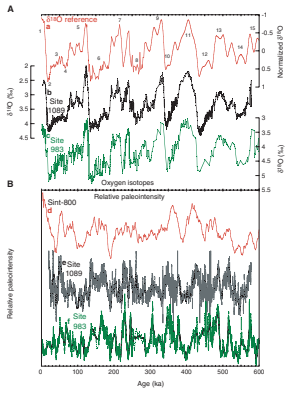

Site 1090

The stratigraphy of the outstanding middle Eocene–lower Miocene section at Site 1090 deserves special mention because it ranks among one of the best deep-sea sections recovered for this time interval. The polarity reversal stratigraphy at Site 1090 is superb and holds much promise for calibrating biostratigraphic and geochemical records to the geomagnetic polarity timescale (GPTS) (Channell et al., in press; Billups et al., 2002). On the basis of calcareous nannofossils, Marino and Flores (2002a) provided evidence for a hiatus or strongly condensed section in the lower Oligocene at Site 1090. Marino and Flores (2002a) placed the Eocene/Oligocene (E/O) boundary at 259 meters composite depth (mcd) and correlated the polarity reversal stratigraphy to the GPTS with the insertion of a cryptochron in C13r. In contrast, planktonic foraminifers point to a continuous record and placement of the E/O boundary at ~269 mcd, although foraminiferal assemblages are poorly preserved across the boundary (Galeotti et al., 2002). On the basis of oxygen isotopic measurements of bulk carbonate and the identification of isotope Event Oi-1 (correlated to Chron 13n) (Zachos et al., 1996), Diekmann et al. (submitted a [N1]) placed the E/O boundary at ~247 mcd and suggested a disconformity in the lower Oligocene. Additional evidence for a lower Oligocene hiatus is provided by multichannel seismic records, which indicate that ~80 m of sediment deposited nearby is missing at Site 1090 (Wildeboer Shut et al., 2002). Channell et al. (in press) provide two alternative interpretations of the polarity reversal stratigraphy at Site 1090 across the Eocene/Oligocene boundary. Option 1 is consistent with the nannofossil biostratigraphy, whereas Option 2 is favored by planktonic foraminiferal stratigraphy. Oxygen and strontium isotope stratigraphy strongly support Option 1, resulting in the identification of a cryptochron within C13r and an apparent hiatus in the early Oligocene affecting the C11n–C11r interval (Channell et al., in press).

Another stratigraphic discrepancy is present below the hiatus at ~70 mcd that removed the lower Pliocene to middle Pliocene section at Site 1090. The section immediately below the hiatus is correlated to Chron C5n near the base of the middle Miocene (Channell et al., in press). This interpretation is supported by strontium, oxygen, and carbon isotope stratigraphy, but is inconsistent with the presence of the planktonic foraminifer *Globorotalia sphericomiozea,* which ranges from the latest Miocene to earliest Pliocene (Galeotti et al., 2002). It is possible

that the section immediately below the hiatus at Site 1090 represents a mixing/reworking zone associated with the unconformity (Channell et al., in press).

PALEOCEANOGRAPHY

Middle Eocene to Early Miocene—Site 1090

One of the central paradigms of Cenozoic climate evolution in the Southern Hemisphere is that Antarctic cooling and ice sheet development was related to the opening of tectonic gateways (Tasmanian Seaway and Drake Passage), which permitted the unrestricted flow of the ACC (Kennett, 1977; Kennett and Barker, 1990). The traditional view is that the Tasmanian Seaway opened sometime near the E/O boundary (Shipboard Scientific Party, 2001) and the Drake Passage opened in the late Oligocene or earliest Miocene (Barker and Burrell, 1977); however, the timing of these events are only loosely constrained because of complex tectonics in both regions (Lawver et al., 1992; Cande et al., 2000). Together with the closure of equatorial gateways and declining atmospheric pCO_2, the development and strengthening of the ACC played an important role in the transition of Earth's climate system from "greenhouse to "icehouse" mode. This transition is expressed in the long-term increase in benthic $\delta^{18}O$ values from the early Eocene to early Oligocene (Fig. F8). Superimposed upon these long-term (tectonic scale) trends in the Cenozoic were quasi-periodic rhythms induced by orbital (Milankovitch) forcing (for review, see Zachos et al., 2001a).

During Leg 177, Paleogene and lowermost Neogene sediments were recovered at only one site. A 330-m-thick section ranging in age from early Miocene to middle Eocene was drilled at Site 1090, located on the southern end of the Agulhas Ridge in the area of an elongated contourite drift body (Wildeboer Schut et al., in press). A clean geomagnetic signal and a verifiably complete composite section make this site an appealing target for paleoceanographic study.

The late Eocene (~35 Ma) has been recognized as a period when multiple meteorites may have impacted the Earth (Glass and Koeberl, 1999). For this reason, Kyte (Chap. 4, this volume) searched the well-dated upper Eocene section of Site 1090 for any evidence of an impact deposit. Concentrations of cosmogenic iridium peak at 950 pg/g in Sample 177-1090B-30X-5, 105–106 cm (291 mcd), providing concrete evidence of an impact event. In addition, both clear and dark-colored spherules were found in samples with the highest Ir and are believed to be microtektites and microkrystites. This event correlates with similar deposits found at ODP Leg 113 Site 689 on the Maud Rise (Glass and Koeberl, 1999) and elsewhere, thereby providing an important time-stratigraphic horizon for long-distance correlation.

Latimer and Filippelli (2002) and Diekmann et al. (submitted a [N1]) produced a large geochemical (bulk sediment parameters), sedimentological (grain size distribution), and clay mineralogical data set to chronicle changes in terrigenous and biogenic fluxes, decipher changes in paleoproductivity, and reconstruct changes in ocean circulation at Site 1090 between ~44 and 17 Ma. On the basis of elevated P/Al ratios, Latimer and Filippelli (2002) identified two intervals of enhanced export production in the South Atlantic during the middle Eocene (44–42 Ma) and across the Eocene–Oligocene transition (Fig. F9). A late Eocene–early Oligocene increase in biogenic export is also indicated by

F8. Composite benthic $\delta^{18}O$ record, p. 38.

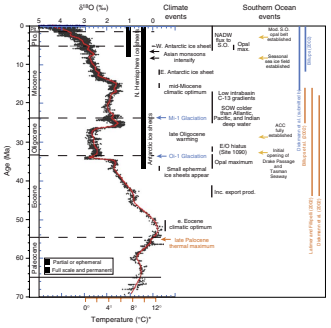

F9. Elemental ratios and total Ba, p. 39.

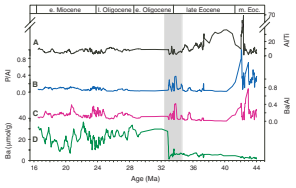

enhanced biogenic opal deposition between 37.5 and 33.5 Ma (Diekmann et al., submitted a [N1]). The latter part of this interval of high opal export was associated with the highest concentration of organic carbon recorded at Site 1090. The late Eocene opal event represents the first significant deposition of biogenic silica at Site 1090, and the timing was similar to increases in silica accumulation reported from the Tasman Rise and Falkland Plateau (Andrews et al., 1975; Ciesielski and Weaver, 1983). At more southerly locations, such as the Maud Rise (Site 689) and the Kerguelen Plateau (Sites 738 and 744), opal accumulation also began in the late Eocene and reached its maximum only after the Eocene/Oligocene boundary (Ehrmann and Mackensen, 1992; Diester-Haass and Zahn, 1996; Salamy and Zachos, 1999). Diekmann et al. (submitted a [N1]) attributed the changes in productivity regime at Site 1090 to paleogeographic changes in the tropical regions that led to increased meridional ocean circulation and the establishment of a more vigorous ACC, including the development of upwelling cells and oceanic frontal systems. They speculated that the late Eocene mass deposition of biogenic opal and organic carbon may have contributed to enhanced consumption of atmospheric CO_2, which served as a positive feedback mechanism for further cooling.

Site 1090 terrigenous proxies indicate a major shift in the composition and style of sedimentation at ~32.8 Ma in the earliest Oligocene (Fig. F9), marking a change from continental to oceanic crustal sources. A possible cause of this shift in source area is a change in circulation that permitted the transport of basaltic material from the rifting region west of Site 1090 in response to the opening of the Drake Passage. The opening of the Tasmanian Gateway to deepwater flow also occurred in the earliest Oligocene (by ~33 Ma), and some geophysical evidence supports a near-synchronous opening of the Drake Passage and Tasmanian Gateway (Lawver et al., 1994; Lawver and Gahagan, 1998). This time was marked by a rapid reduction in siliciclastic sediment supply and the onset of carbonate ooze in Leg 189 cores (Shipboard Scientific Party, 2001). Similar decreases in siliciclastics and increases in biogenic sedimentation occurred near the E/O boundary on the Maud Rise in the South Atlantic (Diester-Haass and Zahn, 1996; Kennett and Barker, 1990; Salamy and Zachos, 1999). Major ice growth began on Antarctica in the earliest Oligocene (Fig. F8) (Zachos et al., 1992) and changed the style of Antarctic continental weathering (Robert and Kennett, 1997). At Site 1090, the clay mineral assemblage changes during the late Eocene to early Oligocene and is marked by an increase in pure terrigenous clay minerals such as illite, chlorite, and kaolinite at the expense of smectite, which appears to be largely of marine origin (Diekmann et al., submitted a [N1]). These changes in terrigenous proxies at Site 1090 are related to global cooling and glaciation that promoted stronger mechanical weathering of continental source areas.

Hopes of obtaining a continuous Paleogene oxygen isotope record at Site 1090 were thwarted by the low abundance and poor preservation of foraminifers, especially across the E/O boundary. Foraminifers were abundant enough, however, for isotope analysis in the upper Oligocene to lower Miocene section. Billups et al. (2002) generated a benthic isotope record from ~25 to 16 Ma at Site 1090, which they correlated to the astronomically tuned $\delta^{18}O$ signal from Site 929 (Fig. F5) (Shackleton et al., 1999). The significance of this correlation lies in the fact that Site 1090 has a geomagnetic polarity reversal stratigraphy, whereas Site 929 does not. Therefore, Site 1090 can potentially be used to fix the geo-

magnetic polarity timescale to the astronomical timescale (Channell et al., in press).

Billups et al. (2002) found that the $\delta^{18}O$ maximum (Mi 1), which is customarily associated with the Oligocene/Miocene (O/M) boundary (Fig. F8), is actually slightly older (23.86 Ma on the timescale of Cande and Kent, 1995) and falls in Subchron C6Cn.2r. The Mi 1 glaciation was probably caused by a "silent node" in Earth's orbital configuration, when low obliquity and low eccentricity resulted in a 200-k.y.-long period of low seasonality (Zachos et al., 2001b). In addition to Mi 1, the O/M boundary is also marked by a maximum in $\delta^{13}C$ values referred to as CM-OM (Hodell and Woodruff, 1994). Billups et al. (2002) found that CM-OM is present only 24 cm above the polarity subchron boundary C6Cn.2n/r at Site 1090 (Fig. F5). Because the O/M boundary is placed at this polarity reversal, the $\delta^{13}C$ maximum is very useful for recognizing the boundary.

Comparison of South Atlantic Site 1090 and tropical North Atlantic Site 929 isotope records reveals no carbon isotope gradient between these sites, whereas $\delta^{18}O$ values of Site 1090 are consistently higher than those at Site 929 (Fig. F5). In fact, there is a general lack of a carbon isotope gradient between the North Atlantic, Southern Ocean (Site 1090), and Pacific Ocean during the majority of the latest Oligocene and early Miocene (Billups et al., 2002). However, a strong oxygen isotopic gradient existed between the Southern Ocean and other ocean basins prior to 17 Ma, suggesting that the deep Southern Ocean was colder and/or more saline than the deep North Atlantic or the Pacific. The relatively cold Southern Ocean reflects a well-developed ACC and deep flow through the Drake Passage by ~26 Ma (Billups et al., 2002).

Middle Miocene to Pliocene

None of the Leg 177 sites contain a continuous section of early middle Miocene age. A hiatus of 14 m.y. duration occurs at Site 1090 at ~70 mcd, extending from the early Miocene to the early Pliocene, whereas basal sediment at Sites 1088 and 1092 date to the middle middle Miocene between ~13 and 14 Ma. Censarek and Gersonde (submitted [N2]) estimated middle to late Miocene thermal gradients across the ACC using diatoms preserved in a latitudinal transect of cores extending from Sites 689 and 690 on Maud Rise (~64.5°S), to Site 1092 on Meteor Rise (47°S), and to Site 1088 on the Agulhas Ridge (41°S). Relatively warm surface water conditions and low latitudinal differentiation persisted until ~13.5 Ma. This is followed by gradual cooling, culminating with the northward expansion of cold waters into the present subantarctic realm centered around 11 Ma, a period of lowest sea level in the Miocene, according to Haq et al. (1987). Although the magnitude of this sea level low stand, which in the absence of Northern Hemisphere ice sheets should indicate expansion of Antarctic ice, is under discussion (Kominz et al., 1998), the co-occurrence of cold surface water expansion and a drop in Southern Ocean bottom-water temperatures (Billups and Schrag, 2002) points to the establishment of the West Antarctic Ice Sheet (WAIS) around the middle/late Miocene boundary. This episode of cooling was followed by a resumption of warmer conditions and decrease of thermal differentiation. However, beginning at ~9 Ma, diatoms that are similar to modern sea ice taxa are present at the Maud Rise sites and then subsequently appear at Site 1092 (Meteor Rise) at ~8 Ma. This pattern may mark the establishment of a seasonal sea ice field and may coincide with the growth of the WAIS.

Billups (2002) produced a preliminary low-resolution benthic isotope record for the upper Miocene through Pliocene section at Site 1088. Although this section was drilled in a single hole only, recovery was better than 95% with gaps only existing at core breaks. Sediment accumulation was slow but apparently continuous from ~12 to 2.5 Ma. Carbon isotopic gradients between the North Atlantic, South Atlantic, and Pacific Oceans indicate that a nutrient-depleted water mass has existed in the South Atlantic since ~6 Ma. Intraocean $\delta^{13}C$ gradients suggest the contribution of Northern Component Water (NCW) was similar to today by 6.0 Ma and greater than today during the early Pliocene. In the late Miocene, benthic $\delta^{18}O$ values at Site 1088 increased in two steps at 7.4 and 6.9 Ma, indicating cooling of intermediate and deepwater masses formed in the Southern Ocean.

Diekmann et al. (submitted b [N3]) compared the sedimentologic histories of the middle Miocene–Pleistocene sections of Site 1088 (41°S) and Site 1092 (46°S) to infer past changes in surface water conditions near the present-day Subtropical Front (Site 1088) and Subantarctic Front (Site 1092), respectively (Fig. F1). Although sediments at both sites are dominantly carbonate ($CaCO_3$ = 90 to 95 wt% at Site 1088 and 60 to 90 wt% at Site 1092), biogenic opal deposition began near the middle/late Miocene boundary at both sites. A switch from nannofossil to foraminiferal oozes and a small opal maximum is recorded at both sites in the latest Miocene and correlates with the global "biogenic bloom" across the Miocene/Pliocene boundary (Dickens and Owen, 1999; Hermoyian and Owen, 2001). Thereafter, the histories of opal deposition at the two sites diverge, indicating a latitudinal decoupling of opal deposition between the northern and southern parts of the Leg 177 transect. At Site 1088 (41°S), carbonate deposition prevailed near the modern Suptropical Front throughout the Pliocene–Pleistocene with an opal peak (up to 6 wt%) in the late Pliocene between 3.1 and 2.2 Ma. This opal maximum at Site 1088 correlates with the early Matuyama Diatom Maximum (MDM) observed to the north at ODP Leg 175 sites in the Namibia upwelling area (Lange et al., 1999).

Sediment at Site 1092 (47°S) contains a higher proportion of biogenic silica than at Site 1088 and is consistent with the formation of the circum-Antarctic opal belt since 2.5 Ma near the modern Polar Front (Diekmann et al., submitted b [N3]). Opal accumulation peaks in the early Pleistocene after 2 Ma at Site 1088 and coincides with an increase in weight percent opal at nearby Site 704 (Froelich et al., 1991). Although poorly recovered, high biogenic silica export during the early Pleistocene is also inferred from the numerous and thick sequences of diatom mats penetrated at Site 1093 (Shipboard Scientific Party, 1999; Pearce et al., submitted [N4]). It is noteworthy that the early Pleistocene diatom maximum between 46° and 50°S in the South Atlantic may have coincided with the end of the MDM off southwest Africa (Lange et al., 1999; Berger et al., 2002), although better chronologic control is needed at Sites 1091 and 1093 to calculate precise opal accumulation rates. These two regions may be linked by production of thermocline water by subduction in the subantarctic region and subsequent upwelling off southwest Africa.

Prior to Leg 177, Site 704 (Leg 114) on Meteor Rise was one of the few sites with sufficient stratigraphic continuity and carbonate content for high-resolution Neogene paleoceanographic studies in the Southern Ocean. Site 1092 was also drilled on Meteor Rise but in shallower water than Site 704 and in an area that was less likely to be affected by downslope transport (Gersonde, Hodell, Blum, et al., 1999). Two related stud-

ies collected stable isotope and ice-rafted debris (IRD) data from the lower and lower upper Pliocene section of Site 1092 and compared the results to those obtained at Site 704 (Andersson et al., 2002; Murphy et al., 2002).

The oxygen and carbon isotope record of Site 1092 is very similar but not identical to the isotope signals at Site 704 (Fig. **F10**) (Andersson et al., 2002). As first noted by Mix et al. (1995), benthic $\delta^{18}O$ values at Site 704 (and Site 1092) are greater than those at deep Pacific Site 849 between 3.5 and 2.7 Ma. This observation is enigmatic because it requires that deep Pacific waters (at a depth of 3850 m) were warmer or less saline than those at a depth of ~2000 to 2500 m in the subantarctic South Atlantic. Nonetheless, the $\delta^{18}O$ results from Site 1092 support those from Site 704 and demonstrate an offset from Pacific values that is often close to 0.3‰–0.5‰ and as high as 0.7‰–0.8‰. Changes in the flux and/or salinity of North Atlantic Deep Water (NADW) do not offer a satisfactory explanation (Andersson et al., 2002), and other mechanisms must be sought to reconcile the Pliocene isotope records from the Southern Ocean and eastern Pacific.

Andersson et al. (2002) also compared benthic $\delta^{13}C$ values at Site 1092 with North Atlantic and deep Pacific end-members (Fig. **F10**). Prior to 3.6 Ma, $\delta^{13}C$ values at Site 1092 were lower, suggesting that the site was bathed by a more nutrient-rich water mass compared to NADW prior to 3.6 Ma. Taken at face value, this contradicts the results of Billups et al. (1998, 2002) suggesting that NADW was as strong or stronger during the early Pliocene than in the Holocene. Either $\delta^{13}C$ gradients between the subantarctic South Atlantic and Pacific Oceans evolved differently than the Atlantic-Pacific gradient (Billups et al., 1998), or benthic $\delta^{13}C$ changes in the Southern Ocean were overprinted by productivity effects (Mackensen et al., 1993).

Benthic $\delta^{13}C$ values at Site 1092 decreased abruptly at 2.75 Ma relative to records in the North Atlantic and Pacific Oceans (Fig. **F11**), which corroborates previous results from Site 704 (Hodell and Ciesielski, 1990; Hodell and Venz, 1992; Raymo et al., 1992). Prior to 2.75 Ma, Southern Ocean benthic $\delta^{13}C$ oscillated between those of the North Atlantic and Pacific Oceans. At ~2.75 Ma, Southern Ocean $\delta^{13}C$ values decreased abruptly, indicating a reduction of deepwater ventilation at the same time as expansion of Northern Hemisphere ice sheets. A progressive reduction of NADW over the past 3 m.y. is also supported by Nd and Pd isotopes in Atlantic ferromanganese crusts (Frank et al., 2002).

In the same set of Site 1092 samples analyzed for stable isotopes, Murphy et al. (2002) documented the occurrence of ice-rafted debris. IRD arrived frequently during the early and early late Pliocene, but only as "background rafting" (occasional grains per sample). The first identifiable IRD above background occurred at MIS KM4 (~3.18 Ma) (Shackleton et al., 1995). Successive IRD peaks become progressively larger thereafter, similar to the pattern noted at nearby Site 704 (Warnke et al., 1992). The greatest IRD peak at 2.8 Ma represents a lag deposit owing to a hiatus. The latest Gauss Chron (~2.8–2.5 Ma) was a time of pronounced change in the subantarctic region that included surface waters cooling, a northward shift of the Polar Front, and establishment of the modern circum-Antarctic opal belt (Fig. **F12**) (Hodell and Ciesielski, 1990; Froelich et al., 1991; Hodell and Venz, 1992). The pattern of IRD delivery to Meteor Rise is also similar to IRD records from the high-latitude North Atlantic (Kleiven et al., 2002), although detailed correlation is required to determine the exact phase relationship. At Site 1092, one

F10. Comparison of benthic $\delta^{18}O$ records, p. 40.

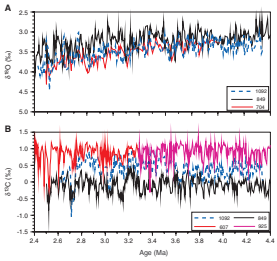

F11. Comparison of benthic $\delta^{13}C$ signals, p. 41.

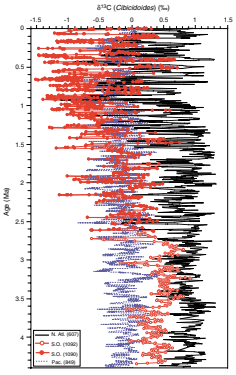

F12. Composite Southern Ocean benthic $\delta^{18}O$ record, p. 42.

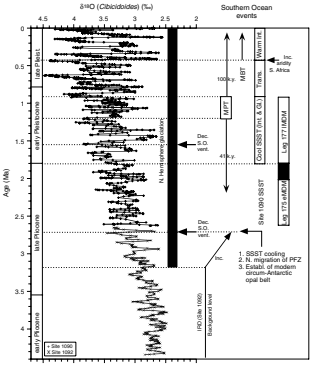

interval in the Gauss Chron and several short intervals in the upper Gilbert Chron are devoid of IRD. Oxygen isotope values at these times were only 0.6‰ less than modern, however (Andersson et al., 2002). These data corroborate a slight warming of deep water during the mid-Pliocene and possible minor deglaciation of Antarctica but do not support speculation of a substantially reduced East Antarctic Ice Sheet.

Pleistocene

One of the main objectives of Leg 177 was to recover expanded sections arrayed across the ACC that could be used to study Pleistocene paleoceanography at orbital and suborbital resolution. For convenience, we review the Pleistocene postcruise contributions under several themes that were elaborated in the original scientific objectives of Leg 177.

Sea-Surface Temperature and Surface Water Structure

The early response of sea-surface temperatures (SSTs) in the Southern Ocean on orbital and suborbital timescales (Imbrie et al., 1992; Charles et al., 1996; Pichon et al., 1992) and the close link between Southern Hemisphere temperature and atmospheric CO_2 (Cuffey and Vimeux, 2001) implicate this region as a potential driver of global climate change. One of the Leg 177 objectives, therefore, was to document Pleistocene SST changes along a north-south transect across the ACC. Summer sea-surface temperatures (SSST) were reconstructed using the modern analog technique (MAT) or paleoecological transfer functions applied to planktonic foraminifers, diatoms, and radiolarian assemblages at four Leg 177 sites (1089, 1090, 1093, and 1094). Changes in surface water density structure were examined by $\delta^{18}O$ analysis of depth-stratified planktonic foraminifers.

Becquey and Gersonde (2002) estimated SSST using planktonic foraminiferal assemblages in core PS2989-2 for the past 550 k.y., and their study was extended to the base of the Pleistocene at nearby subantarctic Site 1090 at millennial resolution (Fig. F13) (Becquey and Gersonde, in press). During the early Pleistocene (1.8–0.9 Ma), relatively cool SSSTs prevailed at 43°S as isotherms in the South Atlantic shifted north by ~7° latitude. This is approximately the same time when thick diatom mats were being deposited farther south at Site 1093 (50°S) (Pearce et al., submitted [N4]). A distinct change in spectral properties began at ~1.2 Ma when the power of the 100-k.y. cycle began to increase. The rather uniform and cold conditions of the early Pleistocene were followed by a transitional period between 0.87 and 0.43 Ma that was marked by increasing SSTs during interglacials. The last 0.4 m.y. was marked by strong variability in SSST with glacial-to-interglacial contrasts up to 8°C. Only during the upper portion of MIS 15 and the earliest parts of MISs 11, 9, 7, 5, and 1 ("climatic optima") do SSSTs exceed those at Site 1090 today. Carbonate dissolution can affect SSST estimates by increasing the relative number of cold-water dwellers (e.g., *Neogloboquadrina pachyderma*) during glacials and warm-water taxa resistant to dissolution (e.g., *Globorotalia inflata*) during warm periods. The latter has been observed during early MIS 11, resulting in an overestimated SSST (Fig. F13).

Cortese and Abelmann (2002) report a 160-k.y.-long record of SSST at centennial resolution derived from a radiolarian-based transfer function at Site 1089 in the northern Subantarctic Zone (Fig. F14). Results indi-

F13. Pleistocene SSST record, p. 43.

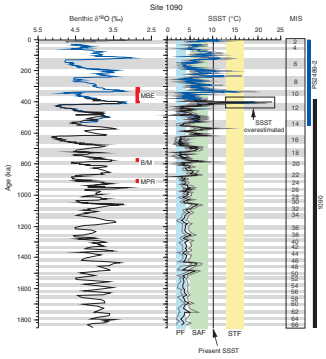

F14. $\delta^{18}O$ of *G. bulloides*, SSST record, atmospheric paleotemperatures, p. 44.

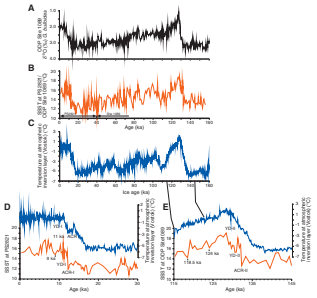

cate a maximum temperature change of up to 7°C in surface waters for the last two glacial terminations (I and II). The rise in SSST precedes changes in oxygen isotopes at both terminations, supporting an early response of Southern Ocean SSST relative to Northern Hemisphere ice volume. Both deglaciations were also interrupted by sudden cooling episodes. Distinct millennial-scale oscillations in temperature occurred during MIS 3 and 4, and SSST changes were almost as great as those observed at terminations. These large SSST variations bear a strong resemblance to planktonic $\delta^{18}O$ changes in the same core (Ninnemann et al., 1999) but differ from the low-amplitude SSST signal (1°–3°C) and warming trend seen after 45 ka in the SSST record estimated by alkenone undersaturation ratios (Sachs et al., 2001). Millennial-scale SSST variations during MISs 3 and 4 at Site 1089 may have been related to rapid movements of the Subtropical Front associated with Dansgaard-Oeschger events. Spectral analysis of SSSTs shows significant power at frequencies observed in the Vostok ice core and North Atlantic sediment cores.

Mortyn et al. (2002) examined changes in surface water column structure over the last two terminations at ODP Sites 1089 and 1093 by measuring the isotopic differences between shallow- and deep-dwelling planktonic foraminifers. During glacial periods, surface water was more stratified south of the Polar Front Zone (PFZ) (Shemesh et al., 2002) and less stratified to the north (Mortyn et al., 2002). Pronounced planktonic $\delta^{13}C$ minima occur on Terminations I and II in deep-dwelling foraminifers at Sites 1089 and 1093. Spero and Lea (2002) have traced carbon isotope minimum events at the last glacial termination to the equatorial Pacific and interpreted them to represent the breakdown of surface stratification in Antarctic surface waters, renewed upwelling of Circumpolar Deep Water (CDW) in the Southern Ocean, and advection of low $\delta^{13}C$ waters to the Subantarctic Front where Antarctic Intermediate Water and Subantarctic Mode Water are formed.

Complementary to the radiolarian-based study of SSST south of the Subtropical Front at Site 1089, Bianchi and Gersonde (2002) reconstructed SSST and sea ice variations across Termination II in Antarctic surface waters, south of the present-day Polar Front. This study is based on diatom records from a longitudinal transect of six piston cores extending from the western Indian Ocean sector into the Scotia Sea and includes the late MIS 6 to MIS 5 sequence recovered at Site 1094. During late MIS 6, cold water from the Weddell Sea extended into the central and eastern South Atlantic and lowered SSST in the present Antarctic Zone to ~0°C. This permitted the expansion of the winter sea ice edge to the position of the modern Polar Front. According to their chronology (Martinson et al., 1987), warming at Termination II started at ~132–131 ka and temperatures increased by ~4°–5°C within a ~3-k.y. period and reached maximum values during earliest MIS 5, lasting for 2–3 k.y. Similar to the record at Site 1089 (Cortese and Abelmann, 2002), the warming at Termination II was punctuated by a major cold reversal. Additional short-lived SSST oscillations occur at 200- to 300-yr intervals and are possibly triggered by short-term meltwater discharges. The SSST pattern during MIS 5e is marked by several fluctuations with amplitudes of 1°–2°C and does not support severe climate instability during MIS 5e as originally proposed on the basis of the Greenland Ice Core Project (GRIP) record (Dansgaard et al., 1993). Applying an age model based on the radiometric dating of the Termination II midpoint at 135 ± 2.5 ka (Henderson and Slowey, 2000), Bianchi and Gersonde (2002) suggested that the onset of warming at Termination II was triggered by precessional changes influencing southern high-latitude sum-

mer insolation. Rapid reduction of the sea ice field and increased SSST may have acted as a positive feedback mechanism by reducing albedo and enhancing ocean-atmosphere gas exchange, thereby releasing CO_2 to the atmosphere. Further reinforcement of the SSST during the termination may be related to changes in global circulation affected by a collapse or strong reduction of NADW production, resulting in additional warming of the southern latitudes.

Kunz-Pirrung et al. (2002) present similar diatom-based studies at and around MIS 11 (Fig. F15), which may have been the warmest and/or longest interglacial of the late Pleistocene. During glacial Stages 10 and 12, the Antarctic Zone, which is currently ice free, was seasonally covered by sea ice. The SSST record obtained at Sites 1093 and 1094 show distinct climate variability at millennial timescales during both cold and warm periods. Termination V is especially noteworthy at Site 1093 because it consists of an 8-m expanded section containing laminated diatom mats (Grigorov et al., 2002). At Termination V (MIS 12/11), SSSTs increased by 4°–6°C but the warming was punctuated by two distinct cooling events at Site 1094 that might be related to meltwater discharges. Maximum temperatures occurred during late Termination V and exceeded modern values by 2°C for a period of 8 k.y. This pattern supports a very early response of SSST in the Southern Ocean to orbital (Milankovitch) forcing. The maximum SSST during the MIS 11 climatic optimum do not exceed values obtained during other interglacial periods such as early MIS 5 or MIS 1, but the total duration of warmth was longer than other interglacials. These results from high-sedimentation-rate cores support the findings of a lower-resolution study of South Atlantic cores by Hodell et al. (2000).

F15. SSST vs. atmospheric temperature, p. 45.

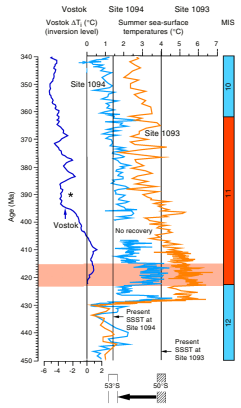

Sea Ice Extent

Sea ice is a fast-changing variable with strong albedo feedback that profoundly affects the physical, chemical, and biological properties of Antarctic surface water and atmospheric circulation. Variations in sea ice also affect the air-sea exchange of gases and may play an important role in glacial-to-interglacial variations in deepwater ventilation and atmospheric pCO_2 (Stephens and Keeling, 2000; Sigman and Boyle, 2000). As such, an important Leg 177 goal was to reconstruct the history, distribution, and seasonal variation of sea ice. One of the few sea ice proxies available is the analysis of sea ice diagnostic taxa of diatoms (Gersonde and Zielinski, 2000).

Shemesh et al. (2002) reconstructed sea ice extent over the last deglaciation in piston core TTN057-13 (Site 1094). High relative abundance of sea ice diatoms during the last glaciation argue for enhanced sea ice cover at this site. Sea ice is the first parameter to change at Termination I, followed by nutrient proxies and SSST. Sea ice decreased abruptly (in ~1000 yr) from 19 to 18 ka and led the increase in atmospheric pCO_2 by ~2000 yr. The early response of Southern Ocean sea ice supports models calling for a role of sea ice in glacial-to-interglacial variations in atmospheric pCO_2 (Moore et al., 2000; Stephens and Keeling, 2000); however, a delay mechanism of a few thousand years may be needed to explain the observed sequence of events.

Kunz-Pirrung et al. (2002) and Bianchi and Gersonde (2002) used diatoms to reconstruct sea ice extent in the Antarctic Zone (including Site 1094) from MIS 6 to MIS 5 and at Sites 1093 and 1094 from MIS 12 to MIS 10, respectively. During glacial Stages 6, 10, and 12, winter sea ice covered the area corresponding to the modern Antarctic Zone and Polar

Front. This is similar to sea ice extent reported for the last glaciation by Crosta et al. (1998) and Gersonde et al. (in press). Cold-water diatom taxa and low biogenic sedimentation rates point to permanent sea ice cover in the area south of 54°S of the Atlantic sector during MIS 6. The winter sea ice edge began to retreat during Terminations II and V at ~132–131 ka and 432 ka, respectively, but advanced again during major cold reversals on both terminations. The central Atlantic sector of the Southern Ocean was ice free throughout the years between ~130 and 110 ka during MIS 5 and between ~425 and 390 ka during MIS 11. Spectral analysis of the diatom sea ice signals reveals distinct millennial-scale cycles including a persistent 3-k.y. periodicity during the mid-Brunhes Chron (Kunz-Pirrung et al., 2002).

Antarctic Ice Sheet Dynamics

Documentation of IRD, including Heinrich Events, in the North Atlantic has contributed greatly to our understanding of Laurentide Ice Sheet dynamics. Is there evidence for millennial-scale variability in Antarctic Ice Sheet similar to that observed for the North Atlantic? To address this question, Kanfoush et al. (2000, 2002) used piston and/or ODP cores at 41°, 47°, and 53°S to reconstruct the distribution of IRD across the PFZ. IRD in the South Atlantic is composed dominantly of ash and quartz with minor amounts of fine-grained volcanics, coarse-crystalline rock fragments, and mica. The source of the volcanic ash is believed to be the South Sandwich Islands in the Scotia arc, with minor contribution from nearby Bouvet Island (Smith et al., 1983). The ash settles on ice shelves and seasonal sea ice and is transported north by tabular icebergs and the seasonal advance of sea ice. Quartz and other nonash lithics are derived mainly from iceberg calving from ice shelves such as those found in the Weddell Sea region.

Kanfoush et al. (2000) found discrete episodes of IRD deposition on millennial timescales throughout the last glaciation (MIS 2 to 4). Prominent IRD layers correlate across the PFZ, suggesting episodes of Antarctic Ice Sheet instability. South Atlantic IRD peaks are associated with times of warming (interstadials) and increased NADW production in the North Atlantic. This interhemispheric linkage may be a manifestation of antiphase climate behavior between these regions (Broecker, 1998; Manabe and Stouffer, 1997). Alternatively, the linking mechanism may have been sea level rise associated with melting of the Laurentide Ice Sheet during strong interstadial events that unpinned grounded Antarctic ice shelves, releasing armadas of icebergs to the South Atlantic. Partial support for this mechanism comes from reported ages of sea level highstands from the Huon Peninsula, New Guinea, and Barbados during MIS 3 (Chappell, 2002) that match the South Atlantic IRD events within chronological uncertainty (Yokoyama et al., 2001; Kanfoush, 2002).

Kanfoush et al. (2002) extended the study of IRD delivery to the South Atlantic at Site 1094 (54°S) over the last four climate cycles (Fig. F16). They found that most, but not all, of the IRD variability is captured by whole-core physical properties such as magnetic susceptibility and gamma ray attenuation bulk density. Each of the last four glacial periods was marked by high IRD abundance and millennial-scale variability that may reflect instability of ice shelves in the Weddell Sea region.

In contrast, the early part of each interglacial period was nearly devoid of IRD, yet its abundance increased during the latter part of each

F16. Correlation of percent ash and sodium concentration, p. 46.

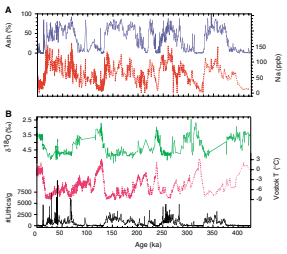

interglacial, marking the onset of a neoglaciation. For the Holocene, Hodell et al. (2001) reported that IRD abundance was very low in piston core TTN057-13 (Site 1094) from 10 to 5.5 ka, coinciding with the early Holocene Hypsithermal. At ~5.5 ka, the delivery of IRD increased abruptly, heralding the onset of neoglacial conditions. This timing is in agreement with an early neoglacial advance of mountain glaciers in South America and New Zealand between 5.4 and 4.9 ka (Porter, 2000). The neoglaciations of MIS 7 and 9 were associated with a substantial increase in planktonic $\delta^{18}O$, whereas the neoglaciation of MIS 5 began prior to the end of the Eemian and was accompanied by only a modest increase in planktonic $\delta^{18}O$ (Kanfoush et al., 2002). Using the SPECMAP age model at Site 1094, the duration of the "IRD-free period" during MIS 11 was longer than any other interglacial of the late Pleistocene (Kanfoush et al., 2002; Hodell et al., in press b).

Kleiven and Jansen (**Chap. 12,** this volume) examined IRD in the early–middle Pleistocene from 0.73 to 1 Ma at Site 1094. This period includes the mid-Pleistocene Transition (MPT) when the dominant power of climate variability shifted from 41- to 100-k.y. cycles. Suborbital variability is present in IRD concentration throughout the middle Pleistocene, and the pacing is similar to that observed for the last glacial period (Kanfoush et al., 2000). This study demonstrates that millennial-scale variability in the South Atlantic was not restricted to the 100-k.y. world but also occurred under glacial conditions with reduced global ice volume. The IRD record at Site 1094 in the early–middle Pleistocene is similar to IRD variability at Site 983 in the North Atlantic, suggesting that the amplitude and pacing of iceberg discharge was similar between the two hemispheres.

Changes in Intermediate and Deepwater Circulation

The South Atlantic sector of the Southern Ocean is a key area for studies of global thermohaline circulation because it represents the insertion point of NADW into Antarctic circumpolar flow (Fig. **F2**). Deep water reflects a mixture of the outflows from all ocean basins. In addition, the process of intermediate and deepwater formation in the Southern Ocean links the atmosphere to the deep sea and the geochemical fingerprint of high-latitude surface waters is transmitted throughout the world's deep ocean. Consequently, changes in the ventilation of deep basins from the Antarctic region could be an important mechanism for atmospheric pCO_2 variation (Toggweiler, 1999; Sigman and Boyle, 2000; Keeling and Stephens, 2001).

The thermohaline "conveyor belt" has undergone large changes during interglacial-to-glacial transitions as production of NADW was reduced and Southern Component Water (SCW) filled the deep Atlantic basins. In the North Atlantic, NADW was replaced by an intermediate water mass (referred to as Glacial North Atlantic Intermediate Water or upper NADW) that extended as far south as 28°S in the western South Atlantic during the last glaciation (Oppo and Horowitz, 2000). How these glacial-to-interglacial changes in North Atlantic circulation affected the Southern Ocean is uncertain because of a fundamental discrepancy in the interpretation of Cd and carbon isotope data in the South Atlantic (for review, see Boyle and Rosenthal, 1996). The Cd content of CDW remained unchanged between glacial and interglacial periods, indicating that thermohaline deepwater circulation in the Southern Ocean was much the same as today. In contrast, glacial benthic $\delta^{13}C$ values in cores from the South Atlantic cores currently

bathed by lower CDW were lower than those in the deep Pacific. Taken at face value, this would imply that the oldest deep water in the ocean was located in the deep South Atlantic and/or the $\delta^{13}C$ in CDW source areas was much lower than today (due to reduced productivity or air-sea exchange). Neither Cd/Ca nor $\delta^{13}C$ is without complication, however. Benthic $\delta^{13}C$ may suffer from productivity overprints (for review, see Mackensen and Bickert, 1999), and Cd is potentially confounded by depth-dependent dissolution (McCorkle et al., 1995).

Although Leg 177 postcruise science has not resolved the "$\delta^{13}C$-Cd controversy," it has made several important contributions toward our understanding of glacial-to-interglacial changes in middepth and deep-water circulation. Venz and Hodell (2002) studied changes in deepwater circulation using benthic $\delta^{13}C$ at Site 1090. This site is near the interface of lower CDW and NADW today. The benthic $\delta^{13}C$ signal at Site 1090 is nearly identical to records at Site 704 and piston core RC13-229, all of which are bathed by CDW. At ~1.55 Ma (MIS 52), glacial $\delta^{13}C$ values at Site 1090 dropped below those in the Pacific, thereby establishing the pattern that persisted throughout the late Pleistocene (Fig. **F11**). Venz and Hodell (2002) speculate that the onset of lower-than-Pacific $\delta^{13}C$ values at Site 1090 may have been related to expansion of the Antarctic sea ice field and reduced ventilation of deep water during glacial periods after 1.55 Ma. This time also marked the onset of a strong 41-k.y. power in all surface and deepwater parameters at Site 704 and tight interhemispheric coupling between the high-latitude North and South Atlantic (Hodell and Venz, 1992).

Hodell et al. (in press a) studied Pleistocene vertical carbon isotope gradients at Sites 1088, 1089, and 1090, which form a depth transect down the northern flank of the Agulhas Ridge (Fig. **F2**). The two deepest Sites 1089 and 1090 (below 3700 m) exhibit large glacial-to-interglacial variations in benthic $\delta^{13}C$, whereas the amplitude of the $\delta^{13}C$ signal at Site 1088 (~2100 m water depth) is much smaller (Fig. **F17**). At no time during the Pleistocene are benthic $\delta^{13}C$ values at Site 1088 lower than the Pacific, indicating that the carbon isotopic signal of middepth waters evolved differently from deep waters in the South Atlantic. Reconstruction of vertical $\delta^{13}C$ gradients for the last glaciation support the existence of a sharp chemocline between 2100 and 2700 m that separated nutrient-depleted middepth waters above 2100 m from poorly ventilated deepwater masses below (Ninnemann and Charles, 2002) (Fig. **F18**). This intermediate-to-deep $\delta^{13}C$ gradient ($\Delta^{13}C_{I-D}$) was pronounced for each glacial stage of the last 1.1 m.y. (Hodell et al., in press a), supporting the existence of a chemical divide in the glacial Southern Ocean separating low-CO_2 middepth water above from high-CO_2 deep water below. Comparison of late Pleistocene variations in $\Delta^{13}C_{I-D}$ and Vostok pCO_2 lends support to the model of Toggweiler (1999) whereby glacial-to-interglacial changes in vertical chemical gradients in the Southern Ocean influence atmospheric pCO_2 (Fig. **F19**).

Diekmann and Kuhn (2002) inferred changes in deepwater circulation using variations in sediment composition and clay mineralogy at Site 1090 over the MPT. The paleoceanographic literature is somewhat contradictory in terms of when the MPT occurred and whether the transition was gradual or abrupt. At Site 1090, spectral changes are first observed at ~1.2 Ma (Fig. **F20**). Clay mineralogical changes indicate that Circumpolar Deep Water expanded farther north during glacials after 1.2 Ma (Diekmann and Kuhn, 2002). This is also supported by isotopic data of Venz and Hodell (2002), who report an increase in the carbon

F17. Benthic $\delta^{13}C$ vs. time and water depth, p. 47.

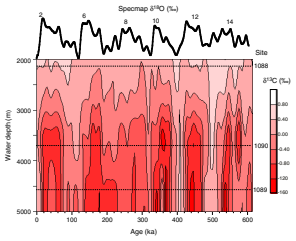

F18. Reconstruction of vertical $\delta^{13}C$ gradients, p. 48.

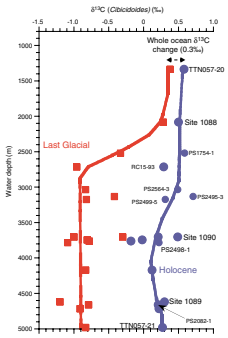

F19. Changes in vertical $\delta^{13}C$ gradients, p. 49.

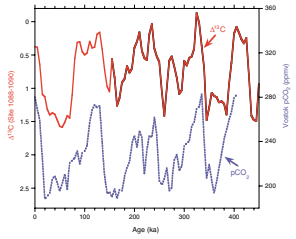

F20. Evolutionary power spectra, p. 50.

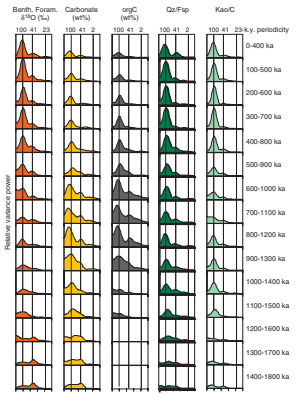

isotopic gradient between Sites 982 and 607 at 1.2 Ma, indicating increased glacial suppression of NCW and farther northward penetration of CDW into the deep North Atlantic. The first prominent 100-k.y. cycle in benthic $\delta^{18}O$ records is often taken to be MIS 22 at ~0.9 Ma. Several important changes occurred at Site 1090 at this time. A change in illite chemistry toward more iron-rich varieties at 0.9 Ma indicates more arid conditions in South African source areas (Diekmann and Kuhn, 2002). At MIS 22, the magnitude and pacing of glacial-to-interglacial variability in benthic $\delta^{13}C$ increased throughout the Atlantic, marking the start of strong 100-k.y. cycles consisting of well-ventilated deep water during interglacials and poorly ventilated deep water during glacials (Venz and Hodell, 2002). The power of the 100-k.y. cycle also increases progressively in the $\Delta^{13}C$ gradient between middepth and deep waters in the South Atlantic between 1.2 and 0.6 Ma (Hodell et al., in press a). The emergence of a strong 100-k.y. cycle in $\Delta^{13}C$ during the mid-Pleistocene is consistent with possible CO_2 forcing of this climate transition.

Kuhn and Diekmann (2002) studied clay minerals at Site 1089 to infer changes in thermohaline circulation on millennial and orbital timescales. During glacial stages, substages, and stadials of the last 600 k.y., they document a fundamental reorganization of the global conveyor system that included a reduction of NADW input to the ACC, as well as a weakening of the return flow of surface waters from the Indian Ocean to the South Atlantic via the Agulhas Current. Grain-size variations indicate stronger contour-current activity during interglacials than during glacial periods in the southern Cape Basin, which may be related to glacial-to-interglacial changes in the production rate of bottom-water masses in source areas within the Weddell Sea.

Carbonate Dissolution

During Leg 177, we used variations in percent color reflectance as a proxy for weight percent $CaCO_3$ and assigned preliminary marine isotope stages assuming that carbonate concentrations were high during interglacial stages and low during glacial stages. This relationship is typical of cores from the Atlantic Ocean. When oxygen isotope measurements were completed postcruise, the "Atlantic-type" carbonate stratigraphy held for all Leg 177 sites except Site 1089, located at 4600 m water depth in the southernmost Cape Basin. Hodell et al. (2001) found the opposite pattern typical instead of Indo-Pacific Ocean cores (i.e., high carbonate during glacial stages and low carbonate during interglacials) (Fig. **F21**). Comparison of weight percent carbonate and foraminiferal fragmentation in the same samples suggests that the carbonate record is controlled mostly by dissolution (Fig. **F22**). The Site 1089 dissolution signal is nearly identical to cores from the Indo-Pacific Ocean but has much greater fidelity because it is free from many of the complications that limit other records (low sedimentation rates, blurring by chemical erosion, bioturbation, etc.). As such, it represents a qualitative, high-resolution record of the temporal evolution of the carbonate saturation state of the deep sea.

Weight percent carbonate lags changes in benthic $\delta^{18}O$ by an average of ~7.6 k.y., and carbonate variations are in phase with the rate of change (first derivative) of benthic $\delta^{18}O$ (Fig. **F21**). Maximum dissolution occurs at the transition from interglacial to glacial periods, and increased preservation occurs during deglaciations. The lagged response

F21. Carbonate and benthic $\delta^{18}O$ signals, p. 51.

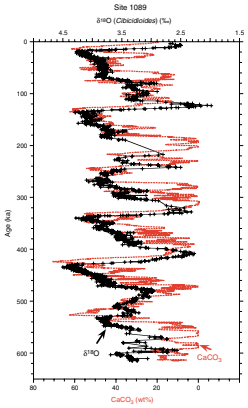

F22. Fragmentation of planktonic foraminifers and carbonate with the CDI, p. 52.

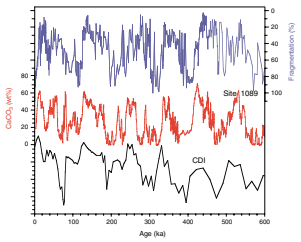

of carbonate to $\delta^{18}O$ reflects a steady-state mass balance process whereby the lysocline adjusts to maintain alkalinity balance between riverine input and marine burial. The Site 1089 carbonate signal is remarkably similar to inferred changes in the Sr/Ca of seawater for the past 250 k.y. (Martin et al., 1999), suggesting that both carbonate dissolution and seawater Sr/Ca may be controlled by sea level–induced changes in the location of carbonate deposition (shelf-basin fractionation) during glacial-to-interglacial cycles (Berger, 1982). The transient change in preservation during the transitions into and out of glacial stages may reflect a response of the carbonate system to a redistribution of alkalinity and dissolved inorganic carbon (DIC) in the ocean (i.e., so-called carbonate compensation by Broecker and Peng, 1987). Comparison of the Site 1089 carbonate and Vostok pCO_2 records suggests a role of deep-sea CO_3^{2-} variations for governing at least some second-order features of the atmospheric pCO_2 signal.

Hodell et al. (in press b) studied the mid-Brunhes dissolution cycle (MBDC) at Sites 1089 and 1090 using stable isotopes and dissolution indices. The MBDC is part of a long-period oscillation that is expressed in dissolution indices and planktonic $\delta^{13}C$ that reach a maximum during MIS 13 and MIS 11. A high correlation between Vostok pCO_2 and percent foraminiferal fragmentation signals between 450 and 300 ka suggests a tight coupling of the marine carbonate system and atmospheric pCO_2 during the mid-Brunhes Chron. MIS 11 is often suggested as a potential analog for Holocene climate change because the Earth's orbital geometry was similar to that of today. Hodell et al. (in press a) caution, however, that the peak in dissolution and $\delta^{13}C$ during the mid-Brunhes Chron indicates that the marine carbonate-carbon cycle was fundamentally different than today. As such, MIS 11 and the Holocene are not entirely analogous.

Marine Sediment–Ice Core Correlations

Ice cores offer the most detailed records available for reconstructing changes in climate and atmospheric composition in the latest Pleistocene. However, many of the mechanisms that control atmospheric composition and climate are rooted in the oceans. The solution to Pleistocene climate problems therefore requires a coupled ocean-atmosphere approach where ice core data are integrated with marine sediment cores. One of the objectives of Leg 177 was to recover expanded upper Pleistocene sections that could be correlated to ice cores from Greenland and Antarctica. A north-south transect of expanded Pleistocene sections was recovered at Sites 1089 (41°S), 1091 (47°S), 1093 (50°S), and 1094 (53°S) that have suitable resolution and continuity for marine sediment–ice core correlation. Postcruise studies have thus far focused mainly on the end-members of the transect (i.e., Sites 1089 and 1094).

Site 1089

Site 1089 is a continuous, 780-k.y.-long sedimentary sequence taken at the same location as piston core RC11-83, which is a benchmark core for climate studies of the high-latitude South Atlantic over the last 80 k.y. Charles et al. (1996) demonstrated that the $\delta^{18}O$ of planktonic foraminifers at this location mimics the δD in the Vostok ice. In addition, benthic $\delta^{13}C$ variations in the same core resemble the oxygen isotope record of Greenland ice cores. The sediment record of Site 1089 can be

correlated, therefore, to two polar ice cores located in opposite hemispheres.

By comparing planktonic $\delta^{18}O$ and benthic $\delta^{13}C$ in the same core, Charles et al. (1996) were able to determine the phase relationship between surface ocean temperature changes in the Southern Ocean and deep-ocean circulation changes controlled by changes in the high-latitude North Atlantic. They found that Northern Hemisphere climate fluctuations lagged those of the Southern Ocean by 1.5 k.y. over the past 80 k.y. This finding was validated by Blunier et al. (1998), who came to nearly the same conclusion by correlating Greenland and Antarctic ice cores using methane fluctuations.

Ninnemann et al. (1999) extended the study of Charles et al. (1996) through the last glacial cycle using ODP Site 1089. They demonstrated that millennial-scale variability in benthic $\delta^{13}C$ could be correlated to $\delta^{18}O$ of the Greenland ice cores, and millennial-scale variability in planktonic $\delta^{18}O$ could be tied to the δD signal in Vostok for the last 120 k.y. (Fig. **F23**). Because expressions of both Greenland and Vostok ice cores are contained in Site 1089 signals, the site offers the opportunity of studying the relative phasing of interhemispheric climate change. Models suggest that SST between the high-latitude North and South Atlantic should be antiphase (Manabe and Stouffer, 1997) because the South Atlantic transports water and heat to the North Atlantic across the equator to balance the water lost due to NADW formation. Broecker (1998) coined this response the "bipolar seesaw." Ninnemann et al. (1999) tested the bipolar seesaw hypothesis using Site 1089. They found a greater poleward extent of warmer surface waters in the South Atlantic with reduced NADW, but it's not straightforward to assess whether the millennial-scale SSTs were actually antiphase. The Site 1089 data are in agreement with at least the sense of the modeling results; however, the phase relationship between thermohaline circulation changes and Southern Hemisphere climate varies at different timescales (e.g., millennial vs. glacial-to-interglacial). Benthic $\delta^{13}C$ at Site 1089 indicates that millennial-scale variability in thermohaline circulation has been a persistent feature of the climate system even during the last interglacial period (MIS 5). Several prominent reductions in NADW occurred during MIS 5, consistent with findings from the North Atlantic (Oppo et al., 2001; Bianchi et al., 2001). This suggests that large ice sheets and meltwater are not always necessary to trigger abrupt changes in the ocean's deep conveyor.

The long Vostok ice core extends back to ~450 ka through the last four climatic cycles (Petit et al., 1999). By correlating millennial-scale oscillation in δD in the Vostok ice core with the $\delta^{18}O$ records of *Globigerina bulloides* and *Neogloboquadrina pachyderma* at Site 1089, Mortyn et al. (submitted [**N5**]) built a marine sediment analog to the Vostok record for the past 400 k.y. In doing so, they developed a new timescale for Vostok that is tied to the orbitally tuned chronology of Site 1089. The chronology is similar to that derived independently by Shackleton (2000) for the Vostok ice core on the basis of tuning the $\delta^{18}O$ of atmospheric oxygen to insolation forcing. The Site 1089–Vostok correlation is used to test the phasing of ocean and atmospheric variables at glacial terminations. As observed in other studies, the minimum values in planktonic $\delta^{18}O$ (warmest surface water temperatures) during terminations led the minimum in benthic $\delta^{18}O$ by several thousands of years, confirming the "lead" of Southern Ocean temperature with respect to ice volume (Imbrie et al., 1992; Charles et al., 1996; Pichon et al., 1992).

F23. Planktonic $\delta^{18}O$ signal with Vostok δD, p. 53.

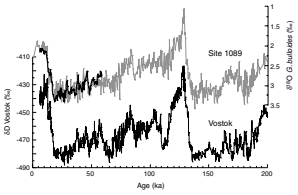

Over the last four terminations, abrupt changes in the chemistry and temperature of the deep Southern Ocean were synchronous with changes in atmospheric pCO_2 and polar air temperatures. This supports a physical rather than biological mechanism for glacial-to-interglacial pCO_2 variations and is consistent with recent models that emphasize the role of sea ice and deep ocean ventilation in controlling atmospheric pCO_2 (Toggweiler, 1999; Stephens and Keeling, 2000; Keeling and Stephens, 2001).

Sites 1093 and 1094

Kanfoush et al. (2002) proposed that Site 1094 could be correlated to Vostok by matching percent ash in South Atlantic sediments with sodium concentrations in Vostok (Fig. **F16**). Both parameters are thought to be influenced by the areal extent of sea ice in the South Atlantic. The correlation yields close agreement between changes in Vostok inferred temperature and the marine $\delta^{18}O$ record on both orbital and millennial timescales. Natural gamma radiation (NGR) at Site 1094 exhibits similarities with dust concentration in Vostok, which originate from the Patagonian region of South America. This may indicate that the NGR signal is controlled by fine-grained terrigenous influx (rich in U and Th) that is transported to Site 1094 by winds.

Kunz-Pirrung et al. (2002) and Bianchi and Gersonde (2002) compared the diatom-based SSST records from Site 1093 (MIS 11 and 10) and Site 1094 (MIS 6 and 5) to Vostok estimated temperature at the level of inversion (ΔT_i) (Fig. **F15**). The two signals are very similar in both shape and amplitude, suggesting that the seasonally ice-free areas south of the Polar Front were a source region of water vapor to the Vostok ice core. SSST estimates during MIS 5 at Site 1094 are in good agreement with Vostok temperature change after correction for deuterium excess (Cuffey and Vimeux, 2001). Ice disturbance near the base of the Vostok ice core has led paleoclimatologists to question whether temperature and pCO_2 estimates are reliable for MIS 11. Correlation of Sites 1093 and 1094 (Kunz-Pirrung et al., 2002), as well as Site 1089 (Hodell et al., in press b), to the Vostok ice core suggests that peak warmth conditions of MIS 11 were captured near the base of the ice core. Peak warmth in both South Atlantic surface waters and Vostok temperatures during MIS 11 were similar to the Holocene, indicating that temperature in the high-latitude Southern Hemisphere during MIS 11 was not substantially warmer than other interglacials of the late Pleistocene (Hodell et al., 2000).

SUMMARY

Here we synthesize Leg 177 results by placing our findings in the historical context of Southern Ocean paleoceanographic evolution. For readability, we omitted references and refer the reader to the detailed discussion and citations in the body of the paper.

The development of the ACC during the Paleogene was a key event in the evolution of the Southern Ocean because it permitted interocean transport among ocean basins and made possible a global thermohaline circulation cell. Its development was closely tied to the opening of tectonic gateways south of Australia (Tasmanian Seaway) and South America (Drake Passage). The timing is only loosely constrained because of complex tectonics in both regions and may be easier to determine by studying Southern Ocean sediments. During Leg 177, we cored a 330-

m-thick section at Site 1090 that ranges in age from the early Miocene to middle Eocene and possesses an excellent geomagnetic polarity reversal stratigraphy. This unique section represents a new Southern Ocean archive of Cenozoic climate change and has led to several important findings regarding the early history of the Southern Ocean:

1. A late Eocene opal maximum was identified between 37.5 and 33.5 Ma that correlates to similar deposits throughout the South Atlantic sector of the Southern Ocean. Increased organic carbon burial associated with this extensive late Eocene opal export may have contributed to a drop in atmospheric pCO_2 and global climatic cooling.
2. A condensed section and/or hiatus at Site 1090 in the early Oligocene (32.8–31.3 Ma) marks the establishment of an unimpeded ACC and formation of dense, cold bottom water along the Antarctic margin.

The opening of the Drake Passage to at least shallow-water flow is inferred at ~33 Ma from increased supply of detrital matter with affinities to oceanic crust derived from rifting west of Site 1090. This timing is near synchronous with the opening of the Tasmanian Seaway between Australia and Antarctica, suggesting circum-Antarctic flow of surface waters by ~33 Ma in the early Oligocene.

A continuous Paleogene isotope record could not be obtained at Site 1090 because of the low abundance and poor preservation of foraminifers in parts of the section; however, a high-resolution record was produced for the upper Oligocene to lower Miocene section (25–16 Ma) and tied to the geomagnetic polarity timescale. Comparison of carbon isotope gradients between the North Atlantic, Southern Ocean (Site 1090), and Pacific Ocean reveals a general lack of a $\delta^{13}C$ gradient among ocean basins during the majority of the latest Oligocene and early Miocene. In contrast, a strong oxygen isotopic gradient existed between the Southern Ocean (Site 1090) and other ocean basins prior to 17 Ma, indicating that the deep Southern Ocean was colder and/or more saline than the deep North Atlantic or the Pacific.

Prior to Leg 177, Site 704 was one of the few sites available for high-resolution Neogene paleoceanographic studies in the Southern Ocean. Site 1092 was drilled on Meteor Rise to improve and complement the existing record at Site 704, located only 34 nmi to the southeast. An enigmatic observation from Site 704 was that benthic $\delta^{18}O$ values were greater than those at deep Pacific Site 849 between 3.5 and 2.7 Ma. This observation is suspicious because it requires that deep Pacific waters (at a depth of 3850 m) were warmer or less saline than those at a depth of ~2000–2500 m in the subantarctic South Atlantic. Benthic $\delta^{18}O$ results from Site 1092 confirm the Site 704 measurements and demonstrate that Southern Ocean $\delta^{18}O$ values were indeed higher than those in the Pacific throughout much of the Pliocene. Changes in the flux and/or salinity of North Atlantic Deep Water do not offer a complete explanation of this observation, and other mechanisms must be sought to reconcile the Pliocene isotope records from the Southern Ocean and eastern Pacific.

The first identifiable IRD above background levels at Site 1092 is present in the late Pliocene at ~3.18 Ma, and IRD peaks become progressively larger thereafter, reaching a maximum at 2.8 Ma. This pattern is similar to the one noted at nearby Site 704 and sites from the high-latitude Northern Hemisphere, suggesting a possible link to the expansion

of Northern Hemisphere ice sheets. The latest Gauss Chron (~2.8–2.5 Ma) was a time of pronounced change in the subantarctic region that included surface waters cooling, a northward shift of the Polar Front, and establishment of the modern circum-Antarctic opal belt.

Pliocene–Pleistocene changes in deepwater circulation have been inferred using benthic $\delta^{13}C$ at Site 1090 (3702 m) and Site 1092 (1974 m). Southern Ocean benthic $\delta^{13}C$ values decreased in two pronounced steps relative to records in the North Atlantic and Pacific. Prior to 2.75 Ma, Southern Ocean benthic $\delta^{13}C$ oscillated between those of the North Atlantic and Pacific. At ~2.75 Ma, Southern Ocean $\delta^{13}C$ values decreased abruptly, indicating a reduction of deepwater ventilation at the same time as expansion of Northern Hemisphere ice sheets. At ~1.55 Ma, benthic $\delta^{13}C$ values dropped below those in the Pacific during glacial periods, thereby establishing a pattern that persisted throughout the late Pleistocene. The onset of "lower-than-Pacific" $\delta^{13}C$ values at Site 1090 may have been related to expansion of the Antarctic sea ice field during glacial periods after 1.55 Ma, which led to a reduction in the ventilation of Southern Component Water.

The carbon isotope signal of middepth Site 1088 (2082 m) evolved differently from deeper sites in the South Atlantic sector of the Southern Ocean during the Pleistocene. At no time during the Pleistocene were benthic $\delta^{13}C$ values at Site 1088 lower than those in the deep Pacific. Reconstruction of vertical $\delta^{13}C$ gradients supports the existence of a sharp chemocline between 2100 and 2700 m during glacial periods of the last 1.1 Ma, which separated nutrient-depleted middepth waters above 2100 m from poorly ventilated deepwater masses below. The vertical carbon isotope gradient between middepth and deep water parallels variations in atmospheric pCO_2 for the last 400 k.y., lending support to changes in Southern Ocean deepwater ventilation as a mechanism of CO_2 change.

Foraminiferal transfer functions at Site 1090 indicate that relatively cool SSSTs prevailed at 43°S during the early Pleistocene (1.8–0.9 Ma) as isotherms in the South Atlantic shifted north by ~7°. To the south, the early Pleistocene is marked by high rates of opal accumulation on Meteor Rise (Site 1092) and thick deposits of diatom mats often containing a near-monospecific diatom assemblage of *Thalassiothrix* sp. At both Sites 1091 (47°S) and 1093 (50°S), the most significant diatom mat sediment was deposited in the late early and mid-Pleistocene. This early Pleistocene diatom maximum between 46° and 50°S in the South Atlantic may bear an inverse relationship to the latest Pliocene (early Matuyama Chron) diatom maximum recorded in Leg 175 sediments off Namibia. The two regions may be linked by production of thermocline water via subduction in the subantarctic region and subsequent upwelling off southwest Africa.

Obtaining a Southern Ocean record of the mid-Pleistocene climate transition was an important objective of Leg 177, which was met at Site 1090. An increase in the 100-k.y. cycle is first observed in power spectra of planktonic foraminiferal SSST, benthic $\delta^{18}O$, and sediment composition at ~1.2 Ma and then intensifies greatly after 0.9 Ma. Clay mineral assemblages at Site 1090 indicate a shift toward more arid conditions in southern Africa at 0.9 Ma. Across the MPT, no change is observed in the pacing or amount of IRD delivered to Site 1094 (53°S). The power of the 100-k.y. cycle increases progressively in the $\delta^{13}C$ gradient between middepth and deep waters in the South Atlantic during the mid-Pleistocene and is consistent with possible CO_2 forcing of this climate transition.

Faunal and isotopic studies provide strong evidence for a mid-Brunhes climate transition in the subantarctic South Atlantic. Beginning with MIS 11, interglacial periods were marked by warmer temperatures and possibly less ice volume than those before 420 k.a. MIS 11 stands out in Leg 177 sediment as the brightest, most carbonate-rich period of the Pleistocene. Diatom-based estimates of SSST indicate that values during the MIS 11 thermal maximum did not exceed those obtained during other interglacials of the past 450 k.y., including the climatic optima of MIS 5 or MIS 1 from the Antarctic Zone. However, the duration of warm conditions was distinctly longer for MIS 11 than any other interglacial, and MIS 11 was also the longest period devoid of IRD in the late Pleistocene.

One unexpected postcruise result was the late Pleistocene carbonate record at Site 1089, which is unlike any other Leg 177 site because it displays a Pacific-type carbonate stratigraphy (i.e., high carbonate glacials and low carbonate interglacials). The Site 1089 carbonate record is controlled by dissolution, and the signal is nearly identical to cores from the Indo-Pacific Ocean. The fidelity of this record is unmatched by other cores, because it is free from many of the complications that limit other records (low sedimentation rates, blurring by chemical erosion, bioturbation, etc.). As such, the Site 1089 carbonate record serves a qualitative, high-resolution proxy of the temporal evolution of the carbonate saturation state of the deep sea.

Expanded late Pleistocene sequences at Sites 1089, 1091, 1093, and 1094 have been used to study the role of the Southern Ocean in glacial-to-interglacial climate change. Several studies have focused on the timing and structure of Southern Ocean changes during the last several deglaciations. Minimum planktonic $\delta^{18}O$ values and increases in SSST estimated by transfer functions lead the minimum in benthic $\delta^{18}O$ by several thousand years at glacial terminations, confirming the "lead" of Southern Ocean temperature with respect to global ice volume. At the highest latitude Site 1094, sea ice is the first parameter to change at Termination I followed by nutrient proxies and SSST. Several terminations are punctuated by significant cold reversals, similar to the Antarctic cold reversal at the last termination, that may be triggered by short-term meltwater discharges from Antarctica.

Sites 1089 and 1094 have been correlated to Greenland and Antarctic ice cores, which permits analysis of the phase relationships between oceanographic and atmospheric variables at glacial terminations. For the last four major deglaciations, changes in the temperature and chemistry of the deep Southern Ocean were synchronous with changes in polar air temperatures and atmospheric CO_2 recorded in the Vostok ice core. This relationship supports a physical mechanism for glacial-to-interglacial pCO_2 variations and is consistent with recent models that emphasize the role of sea ice and deep ocean ventilation in controlling atmospheric pCO_2.

Much effort has been devoted to studying millennial-scale variability in the high-latitude North Atlantic, and Leg 177 sediments now allow us to extend these studies to the South Atlantic sector of the Southern Ocean. At Site 1089, radiolarian-based estimates of SSST indicate very large millennial-scale changes in SSST during MIS 3 and MIS 4 that are almost as great as those observed at Terminations I and II. Millennial-scale variability in the delivery of IRD, consisting mostly of quartz and ash, were found to coincide across the Polar Front from Sites 1089 (41°S) to Site 1094 (53°S) during MIS 3. South Atlantic IRD peaks are as-

sociated with times of warming (interstadials) and increased NADW production in the North Atlantic, suggesting an antiphase relationship between these regions. The linking mechanism may have been sea level rise associated with melting of the Laurentide Ice Sheet during strong interstadial events that unpinned grounded Antarctic ice shelves, releasing armadas of icebergs to the South Atlantic.

Millennial-scale variability in SSST and IRD was not limited to the last glacial period. At Site 1094, sub-Milankovitch variability in IRD occurred during glacial periods for the past 1 m.y., with a pacing similar to that of the last glacial period. Over the last four climate cycles, the early part of each interglacial period was marked by low IRD abundance during hypsithermal conditions, followed by the cooling and the resumption of IRD delivery during the onset of neoglaciations.

CONCLUSION

A number of exceptional postcruise studies have resulted from ODP Leg 177 thus far and have advanced our goal of documenting the paleoceanographic history of the southeast Atlantic sector of the Southern Ocean on tectonic to millennial timescales. Here, we have summarized the results that have been produced in the 4 yr elapsed since Leg 177. Many exciting results are forthcoming from ongoing studies, and we are confident that the superb sediments recovered during Leg 177 will serve as raw material for paleoceanographic research for years to come. One of the rationales for drilling Leg 177 sites was the relative paucity of sedimentary sequences available from the Southern Ocean that were suitable for high-resolution paleoceanographic studies. Although Leg 177 fills a critical gap in the distribution of Southern Ocean sites, we emphasize the need to drill additional north-south transects across the ACC in different sectors of the Southern Ocean. The Antarctic circumpolar region covers a wide area and studies of piston cores from the last glacial period indicate that other sectors of the Southern Ocean may have responded differently than the Atlantic (Ninnemann and Charles, 1997). These results underscore the need for additional drilling in the high southern latitudes, and we look forward to a speedy return of the riserless drilling vessel to the Southern Ocean under the new Integrated Ocean Drilling Program (IODP).

ACKNOWLEDGMENTS

None of this research would have been possible without the dedication and hard work of the crew, marine technicians, and scientific party of Leg 177. We thank Leg 177 scientists for making available to us their published and unpublished results for this synthesis; however, all errors in recitation or integration of individual results are our own. R. Tiedemann and an anonymous reviewer made valuable suggestions for improvement of the manuscript. This research used samples and/or data provided by the Ocean Drilling Project (ODP). ODP is sponsored by the U.S. National Science Foundation (NSF) and participating countries under management of Joint Oceanographic Institutions (JOI), Inc. Preparation of this synthesis chapter was supported by the NSF (Grant OCE-99007036) to D.H. and funding from the Deutsche Forschungsgemeinschaft (DFG Grant Ge516/6) to R.G.

REFERENCES

Andersson, C., Warnke, D., Channell, J.E.T., Stoner, J., and Jansen, E., 2002. The mid-Pliocene (4.3–2.6 Ma) benthic stable isotope record from the Southern Ocean: ODP Sites 1092 and 704, Meteor Rise. *Palaeogeogr., Palaeoclimatol., Palaeoecol.,* 182:165–181.

Andrews, P.B, Goston, V.A., Hampton, M.A., Margolis, S.V., and Ovenshine, A.T., 1975. Synthesis—sediments of the Southwest Pacific Ocean, Southeast Indian Ocean, and South Tasman Sea. *In* Kennett, J.P., Houtz, R.E. et al., *Init. Repts. DSDP,* 29: Washington (U.S. Govt. Printing Office), 1147–1153.

Barker, P.F., and Burrell, J., 1977. The opening of the Drake Passage. *Mar. Geol.,* 25:15–34.

Becquey, S., and Gersonde, R., in press. A 0.55-Ma paleotemperature record from the subantarctic zone: implications for antarctic circumpolar current development. *Paleoceanography.*

————, 2002. Past hydrographic and climatic change in the subantarctic zone of the South Atlantic—the Pleistocene record from ODP Site 1090. *Palaeogeogr., Palaeoclimatol., Palaeoecol.,* 182:221–239.

Berger, W.H., 1982. Deglacial CO_2 buildup: constraints on the coral-reef model. *Palaeogeogr. Palaeoclimatol. Palaeoecol.*, 40:235–253.

Berger, W.H., Lange, C.B., and Pérez, M.E., 2002. The early Matuyama Diatom Maximum off SW Africa: a conceptual model. *Mar. Geol.,* 180:105–116.

Bianchi, C., and Gersonde, R., 2002. The Southern Ocean surface between marine isotope Stages 6 and 5d: shape and timing of climate changes. *Palaeogeogr., Palaeoclimatol., Palaeoecol.,* 187:151–177.

Bianchi, G.G., Vautravers, M., and Shackleton, N.J., 2001. Deep flow variability under apparently stable North Atlantic Deep Water production during the last interglacial of the subtropicalal NW Atlantic. *Paleoceanography,* 13:84–95.

Billups, K., 2002. Late Miocene through early Pliocene deep water circulation and climate change viewed from the sub-Antarctic South Atlantic. *Palaeogeogr., Palaeoclimatol., Palaeoecol.,* 185:287–307.

Billups, K., Channell, J., and Zachos, J., 2002. Late Oligocene to early Miocene paleoceanography from the subantarctic South Atlantic (ODP Leg 177). *Paleoceanography,* 17:10.1029/2000PA000568.

Billups, K., Ravelo, A.C., and Zachos, J.C., 1998. Early Pliocene deep water circulation in the western equatorial Atlantic: implications for high-latitude climate change. *Paleoceanography,* 13:84–95.

Billups, K., and Schrag, D.P., 2002. Paleotemperature and ice volume of the past 27 Myr revisited with paired Mg/Ca and $^{18}O/^{16}O$ measurements on benthic foraminifera. *Paleoceanography,* 17:10.1029/2000PA000567.

Blunier, T., Chappellaz, J., Schwander, J., Dällenbach, A., Stauffer, B., Stocker, T.F., Raynaud, D., Jouzel, J., Clausen, H.B., Hammer, C.U., and Johnson, S.J., 1998. Asynchrony of Antarctic and Greenland climate change during the last glacial period. *Nature,* 394:739–743.

Boyle, E.A., and Rosenthal, Y., 1996. Chemical hydrography of the South Atlantic during the last glacial maximum: Cd vs. $\delta^{13}C$. *In* Wefer, G., Berger, W.H., Siedler, G., and Webb, D. (Eds.), *The South Atlantic: Present and Past Circulation:* Berlin (Springer), 423–443.

Broecker, W.S., 1998. Paleocean circulation during the last deglaciation: a bipolar seesaw? *Paleoceanography,* 13:119–121.

Broecker, W.S., and Peng, T.-H., 1987. The role of $CaCO_3$ compensation in the glacial to interglacial atmospheric CO_2 change. *Global Biogeochem. Cycles,* 1:15–29.

Cande, S.C., and Kent, D.V., 1995. A new geomagnetic polarity time scale for the late Cretaceous and Cenozoic. *J. Geophys. Res.,* 97:13917–13951.

Cande, S.C., Stock, J.M., Muller, R.D., and Ishihara, T., 2000. Cenozoic motion between east and west Antarctica. *Nature,* 404:145–150.

Censarek, B., and Gersonde, R., 2002. Miocene diatom biostratigraphy at ODP Sites 689, 690, 1088, 1092 (Atlantic sector of the Southern Ocean). *Mar. Micropaleontol.,* 45:309–356.

Channell, J.E.T., Galeotti, S., Martin, E.E., Billups, K., Scher, H., and Stoner, J.S., in press. Eocene to Miocene magnetic, bio- and chemostratigraphy at ODP Site 1090 (subantarctic South Atlantic). *Geol. Soc. Am. Bull.*

Channell, J.E.T., and Stoner, J.S, 2002. Plio–Pleistocene magnetic polarity stratigraphies and diagenetic magnetite dissolution at ODP Leg 177 Sites (1089, 1091, 1093, and 1094). *Mar. Micropaleontol.,* 45:269–290.

Channell, J.E.T., Stoner, J.S., Hodell, D.A., and Charles, C.D., 2000. Geomagnetic paleointensity for the last 100 kyr from the sub-antarctic South Atlantic: a tool for inter-hemispheric correlation. *Earth Planet. Sci. Lett.,* 175:145–160.

Chappell, J., 2002. Sea level changes forced ice breakouts in the last glacial cycle: new results from coral terraces. *Quat. Sci. Rev.,* 21:1229–1240.

Charles, C.D., and Fairbanks, R.G., 1992. Evidence from Southern Ocean sediments for the effect of North Atlantic deep-water flux on climate. *Nature,* 355:416–419.

Charles, C.D., Lynch-Stieglitz, J., Ninnemann, U.S., and Fairbanks, R.G., 1996. Climate connections between the hemispheres revealed by deep sea sediment core/ice core correlations. *Earth Planet. Sci. Lett.,* 142:19–27.

Ciesielski, P.F., and Weaver, F.M., 1983. Neogene and Quaternary paleoenvironmental history of Deep Sea Drilling Project Leg 71 sediments, southwest Atlantic Ocean. *In* Ludwig, W.J., Krasheninnikov, V.A., et al., *Init. Repts. DSDP,* 71 (Pt. 1): Washington (U.S. Govt. Printing Office), 461–477.

Cortese, G., and Abelmann, A., 2002. Radiolarian-based paleotemperatures during the last 160 k.y.s. at ODP Site 1089 (Southern Ocean, Atlantic Sector). *Palaeogeogr., Palaeoclimatol., Palaeoecol.,* 182:259–286.

Crosta, X., Pichon, J.-J., and Burckle, L.H., 1998. Application of modern analog technique to marine Antarctic diatoms: reconstruction of maximum sea-ice extent at the Last Glacial Maximum. *Paleoceanography,* 13:284–297.

Cuffey, K.M., and Vimeux, F., 2001. Covariation of carbon dioxide and temperature from the Vostok ice core after deuterium-excess correction. *Nature,* 412:523–526.

Dansgaard, W., Johnsen, S.J., Clausen, H.B., Dahl-Jensen, D., Gundestrup, N.S., Hammer, C.U., Hvidberg, C.S., Steffensen, J.P., Sveinbjörnsdottir, A.E., Jouzel, J., and Bond, G., 1993. Evidence for general instability of past climate from a 250-kyr ice-core record. *Nature,* 364:218–220.

Dickens, G.R., and Owen, R.M., 1999. The latest Miocene–early Pliocene biogenic bloom: a revised Indian Ocean perspective. *Mar. Geol.,* 161:75–91.

Diekmann, B., and Kuhn, G., 2002. Sedimentary record of the mid-Pleistocene climate transition in the southeastern South Atlantic (ODP Site 1090). *Palaeogeogr., Palaeoclimatol., Palaeoecol.,* 182:241–258.

Diester-Haass, L., and Zahn, R., 1996. Eocene–Oligocene transition in the Southern Ocean: history of water mass circulation and biological productivity. *Geology,* 24:163–166.

Ehrmann, W.U., and Mackensen, A., 1992. Sedimentological evidence for the formation of an East Antarctic ice sheet in Eocene/Oligocene time. *Palaeogeogr., Palaeoclimatol., Palaeoecol.,* 93:85–112.

Evans, H.F., and Channell, J.E.T., in press. Upper Miocene magnetic stratigraphy from ODP Site 1092 (sub-Antarctic South Atlantic): recognition of "cryptochrons" in C5n. *Geophys. J. Int.*

Flores, J.A., and Marino, M., 2002. Pleistocene calcareous nannofossil stratigraphy for ODP Leg 177 (Atlantic sector of the Southern Ocean). *Mar. Micropaleontol.,* 45:191–224.

Frank, M., Whiteley, N., Kasten, S., Hein, J.R., and O'Nions, K., 2002. North Atlantic Deep Water export to the Southern Ocean over the past 14 Myr: evidence from Nd

and Pb isotopes in ferromanganese crusts. *Paleoceanography,* 17:10.1029/2000PA000606.

Froelich, P.N., Malone, P.N., Hodell, D.A., Ciesielski, P.F., Warnke, D.A., Westall, F., Hailwood, E.A., Nobes, D.C., Fenner, J., Mienert, J., Mwenifumbo, C.J., and Müller, D.W., 1991. Biogenic opal and carbonate accumulation rates in the subantarctic South Atlantic: the late Neogene of Meteor Rise Site 704. *In* Ciesielski, P.F., Kristoffersen, Y., et al., *Proc. ODP, Sci. Results,* 114: College Station, TX (Ocean Drilling Program), 515–550.

Galeotti, S., Cocciono, R., and Gersonde, R., 2002. Middle Eocene–early Pliocene planktic foraminiferal biostratigraphy at ODP Leg 177 Site 1090, Agulhas Ridge. *Mar. Micropaleontol.,* 45:357–381.

Gersonde, R., Abelmann, A., Brathauer, U., Becquey, S., Bianchi, C., Cortese, G., Grobe, H., Kuhn, G., Niebler, H.-S., Segl, M., Zielinski, U., and Fuetterer, D.K., in press. Last glacial sea-surface temperatures and sea-ice extent in the Southern Ocean (Altantic-Indian sector)—a multiproxy approach. *Paleoceanography* (GLAMAP 2000 issue).

Gersonde, R., and Hodell, D.A., 2002. Southern Ocean paleoceanography—insights from Ocean Drilling Program Leg 177. *Palaeogeogr., Palaeoclimatol., Palaeoecol.,* 182:145–149.

Gersonde, R., Hodell, D.A., Blum, P., et al., 1999. *Proc. ODP, Init. Repts.,* 177 [CD-ROM]. Available from: Ocean Drilling Program, Texas A&M University, College Station, TX 77845-9547, U.S.A.

Gersonde, R., and Zielinski, U., 2000. The reconstruction of late Quaternary Antarctic sea-ice distribution—the use of diatoms as a proxy for sea-ice. *Palaeogeogr., Palaeoclimatol., Palaeoecol.,* 162:263–286.

Glass, B.P., and Koeberl, C., 1999. Ocean Drilling Project Hole 689B spherules and upper Eocene microtektite and clinopyroxene-bearing spherule strewn fields. *Meteoritics Planet. Sci.,* 34:185–196.

Grigorov, I., Pearce, R.B., and Kemp, A.E.S., 2002. Southern Ocean laminated diatom ooze: mat deposits and potential for palaeo-flux studies, ODP Leg 177, Site 1093. *Deep-Sea Res*., 49:3391–3407.

Guyodo, Y., and Valet, J.P., 1999. Global changes in intensity of the Earth's magnetic field during the past 800 kyr. *Nature,* 399:249–252.

Haq, B.U., Hardenbol, J., and Vail, P.R., 1987. Chronology of fluctuating sea levels since the Triassic. *Science,* 235:1156–1167.

Henderson, G.M., and Slowey, N.C., 2000. Evidence from U-Th dating against Northern Hemisphere forcing of the penultimate deglaciation. *Nature,* 404:61–66.

Hermoyian, C.S., and Owen, R.M., 2001. Late Miocene–early Pliocene biogenic bloom: evidence from low-productivity regions of the Indian and Atlantic Oceans. *Paleoceanography,* 16:95–100.

Hodell, D.A., Charles, C.D., and Ninnemann, U.S., 2000. Comparison of interglacial stages in the South Atlantic sector of the southern ocean for the past 450 kyr: implications for marine isotope stage (MIS) 11. *Global Planet. Change,* 24:7–26.

Hodell, D.A., Charles, C.D., Ninnemann, U.S., and Venz, K.A., in press a. Pleistocene vertical carbon isotope gradients in the South Atlantic sector of the Southern Ocean. *Geochem., Geophys., Geosyst.*

Hodell, D.A., Charles, C.D., and Sierro, F.J., 2001. Late Pleistocene evolution of the ocean's carbonate system. *Earth Planet. Sci. Lett.,* 192:109–124.

Hodell, D.A., Kanfoush, S., Shemesh, A., Crosta, X., Charles, C.D., and Guilderson, T.P., 2001. Abrupt cooling of Antarctic surface waters and sea ice expansion in the South Atlantic sector of the Southern Ocean at 5000 cal yr B.P. *Quat. Res.,* 56:191–198.

Hodell, D.A., Kanfoush, S.L., Venz, K.A., Charles, C.D., and Sierro, F.J., in press b. The mid-Brunhes transition in ODP sites 1089 and 1090. *In* Droxler, A. (Ed.), *Marine Isotope Stage 11: An Extreme Interglacial,* Am. Geophys. Union, Geophys. Monogr. Ser.

Hodell, D.A., and Ciesielski, P.F., 1990. Southern Ocean response to the intensification of Northern Hemisphere glaciation at 2.4 Ma. *In* Bleil, U., and Thiede, J. (Eds.), *Geological History of the Polar Oceans: Arctic versus Antarctic:* Dordrecht (Kluwer), 707–728.

Hodell, D.A., and Venz, K., 1992. Toward a high-resolution stable isotopic record of the Southern Ocean during the Pliocene–Pleistocene (4.8 to 0.8 Ma). *In* Kennett, J.P., Warnke, D.A. (Eds.), *The Antarctic Paleoenvironment: A Perspective on Global Change* (Pt. 1). Am. Geophys. Union, Antarct. Res. Ser., 56:265–310.

Hodell, D.A., and Woodruff, F., 1994. Variations in the strontium isotopic ratio of seawater during the Miocene: stratigraphic and geochemical implications. *Paleoceanography,* 9:405–426.

Imbrie, J., Boyle, E.A., Clemens, S.C., Duffy, A., Howard, W.R., Kukla, G., Kutzbach, J., Martinson, D.G., McIntyre, A., Mix, A.C., Molfino, B., Morley, J.J., Peterson, L.C., Pisias, N.G., Prell, W.L., Raymo, M.E., Shackleton, N.J., and Toggweiler, J.R., 1992. On the structure and origin of major glaciation cycles, 1. Linear responses to Milankovitch forcing. *Paleoceanography,* 7:701–738.

Kanfoush, S.L., 2002. Millennial-scale variability in late Pleistocene ice-rafting to the South Atlantic Ocean [Ph.D. dissert.]. Univ. Florida, Gainesville.

Kanfoush, S.L., Hodell, D.A., Charles, C.D., Guilderson, T.P., Mortyn, P.G., and Ninnemann, U.S., 2000. Millennial-scale instability of the Antarctic ice sheet during the last glaciation. *Science,* 288:1815–1818.

Kanfoush, S.L., Hodell, D.A., Charles, C.D., and Janecek, T.R., 2002. Comparison of ice-rafted debris and physical properties in ODP Site 1094 (South Atlantic) with the Vostok ice core over the last three climate cycles. *Palaeogeogr., Palaeoclimatol., Palaeoecol.,* 182:329–349.

Keeling, R.F., and Stephens, B.B., 2001. Antarctic sea ice and the control of Pleistocene climate instability. *Paleoceanography,* 16:112–131.

Kennett, J.P., 1977. Cenozoic evolution of Antarctic glaciation, the circum-Antarctic Ocean, and their impact on global paleoceanography. *J. Geophys. Res.,* 82:3843–3860.

Kennett, J.P., and Barker, P.F., 1990. Latest Cretaceous to Cenozoic climate and oceanographic developments in the Weddell Sea, Antarctica: an ocean-drilling perspective. *In* Barker, P.F., Kennett, J.P., et al., *Proc. ODP, Sci. Results,* 113: College Station, TX (Ocean Drilling Program), 937–960.

Kleiven, H.F., Jansen, E., Fronval, T., and Smith, T.M., 2002. Intensification of Northern Hemisphere glaciations in the circum Atlantic region (3.5–2.4 Ma)—ice-rafted detritus. *Palaeogeogr., Palaeoclimatol., Palaeoecol.,* 184:213–223.

Kominz, M.A., Miller, K.G., and Browning, J.V., 1998. Long-term and short-term global Cenozoic sea-level estimates. *Geology,* 26:311–314.

Kroopnick, P., 1985. The distribution of ^{13}C of pCO_2 in the world oceans. *Deep-Sea Res. Part A,* 32:57–84.

Kuhn, G., and Diekmann, B., 2002. Late Quaternary variability of ocean circulation in the southeastern South Atlantic inferred from the terrigenous sediment record of a drift deposit in the southern Cape Basin (ODP Site 1089). *Palaeogeogr., Palaeoclimatol., Palaeoecol.,* 182:287–303.

Kunz-Pirrung, M., Gersonde, R., and Hodell, D.A., 2002. Mid-Brunhes century-scale diatom sea surface temperature and sea ice records from the Atlantic sector of the Southern Ocean (ODP Leg 177, Sites 1093, 1094 and core PS 2089-2). *Palaeogeogr., Palaeoclimatol., Palaeoecol.,* 182:305–328.

Lange, C.B., Berger, W.H., Lin, H.-L., Wefer, G., and Shipboard Scientific Party, 1999. The early Matuyama diatom maximum off SW Africa, Benguela Current System (ODP Leg 175). *Mar. Geol.,* 161:93–114.

Latimer, J.C., and Filippelli, G.M., 2002. Eocene to Miocene terrigenous inputs, paleoproductivity, and the onset of the ACC: geochemical evidence from ODP Leg 177, Site 1090. *Palaeogeogr., Palaeoclimatol., Palaeoecol.,* 182:151–164.

Lawver, L.A., and Gahagan, L.M., 1998. Opening of Drake Passage and its impact on Cenozoic ocean circulation. *In* Crowley, T.J., and Burke, K.C. (Eds.), *Tectonic Boundary Conditions for Climate Reconstructions*. Oxford Monogr. Geol. Geophys.: Oxford, UK (Oxford Univ. Press), 39:212–223.

Lawver, L.A., Gahagan, L.M., and Coffin, M.F., 1992. The development of paleoseaways around Antarctica. *In* Kennett, J.P., and Warnke, D.A. (Eds.), *The Antarctic Paleoenvironment: A Perspective on Global Change (Pt. 1)*. Am. Geophys. Union, Antarct. Res. Ser., 56:7–30.

Lawver, L.A., Williams, T., and Sloan, B.J., 1994. Seismic stratigraphy and heat flow of Powell Basin. *Terra Antarct.*, 1:309–310.

Levitus, S., and Boyer, T.P., 1994. *World Ocean Atlas 1994* (Vol. 4): *Temperature*. NOAA Atlas NESDIS 4.

Mackensen, A., and Bickert, T., 1999. Stable carbon isotopes in benthic foraminifera: proxies for deep and bottom water circulation and new production. *In* Fischer, G., and Wefer, G. (Eds.), *Use of Proxies in Paleoceanography:* Berlin Heidelberg (Springer Verlag), 229–254.

Mackensen, A., Hubberten, H.W., Bickert, T., Fischer, G., Futterer, D.K., 1993. The ^{13}C in benthic foraminiferal tests of *Fontbotia wuellerstorfi* (Schwager) relative to the ^{13}C of dissolved inorganic carbon in Southern Ocean deep water: implications for glacial ocean circulation models. *Paleoceanography,* 8:587–610.

Mackensen, A., Rudolph, M., and Kuhn, G., 2001. Late Pleistocene deep-water circulation in the subantarctic eastern Atlantic. *Global Planet. Change*, 30:197–229.

Manabe, S., and Stouffer, R.J., 1997. Coupled ocean-atmosphere model response to freshwater input: comparison to Younger Dryas event. *Paleoceanography*, 12:321–336.

Marino, M., and Flores, J.A., 2002a. Middle Eocene to Early Oligocene calcareous nannofossil stratigraphy at Leg 177 Site 1090. *Mar. Micropaleontol.,* 45:383–398.

————, 2002b. Miocene to Pliocene calcareous nannofossil biostratigraphy at ODP Leg 177 Sites 1088 and 1090. *Mar. Micropaleontol.,* 45:291–307.

Martin, P.A., Lea, D.W., Mashiotta, T.A., Papenfuss, T., and Sarnthein, M., 1999. Variation of foraminiferal Sr/Ca over Quaternary glacial–interglacial cycles: evidence for changes in mean ocean Sr/Ca? *Geochem. Geophys. Geosyst.,* 1:1999GC000006.

Martinson, D.G., Pisias, N.G., Hays, J.D., Imbrie, J., Moore, T.C., and Shackleton, N.J., 1987. The orbital theory of Pleistocene climate: support from a revised chronology of the marine ^{18}O record. *In* Berger, A., Imbrie, J., Hays, J., Kukla, G., and Saltzman, B. (Eds.), *Milankovitch and Climate, Part I*: Dordrecht (D. Reidel), 269–305.

McCorkle, D.C., Martin, P.A., Lea, D.C., and Klinkhammer, G.P., 1995. Evidence of a dissolution effect on benthic foraminifera shell chemistry: $\delta^{13}C$, Cd/Ca, Ba/Ca, and Sr/Ca results from the Ontong Java Plateau. *Paleoceanography,* 10:699–714.

Miller, K.G., Wright, J.D., and Fairbanks, R.G., 1991. Unlocking the Ice House: Oligocene–Miocene oxygen isotopes, eustasy, and margin erosion. *J. Geophys. Res.,* 96:6829–6848.

Mix, A.C., Pisias, N.G., Rugh, W., Wilson, J., Morey, A., and Hagelberg, T.K., 1995. Benthic foraminifer stable isotope record from Site 849 (0–5 Ma): local and global climate changes. *In* Pisias, N.G., Mayer, L.A., Janecek, T.R., Palmer-Julson, A., and van Andel, T.H. (Eds.), *Proc. ODP, Sci. Results,* 138: College Station, TX (Ocean Drilling Program), 371–412.

Moore, J.K., Abbott, M.R., Richman, J.G., and Nelson, D.M., 2000. The Southern Ocean at the Last Glacial Maximum: a strong sink for atmospheric CO_2. *Global Biogeochem. Cycles,* 14:455–475.

Mortyn, P.G., Charles, C.D., and Hodell, D.A., 2002. Southern Ocean upper water column structure over the last 140 k.y. with emphasis on glacial terminations. *Global Planet. Change,* 34:241–252.

Murphy, L., Warnke, D.A., Andersson, C., Channell, J., and Stoner, J., 2002. History of ice rafting at South Atlantic ODP Site 177-1092 during the Gauss and the late Gilbert Chron. *Palaeogeogr., Palaeoclimatol., Palaeoecol.,* 182:183–196.

Ninnemann, U.S., and Charles, C.D., 1997. Regional differences in Quaternary subantarctic nutrient cycling: link to intermediate and deep water ventilation. *Paleoceanography,* 12:560–567.

————, 2002. Changes in the mode of Southern Ocean circulation over the last glacial cycle revealed by foraminiferal stable isotope variability. *Earth Planet. Sci. Lett.,* 201:383–396.

Ninnemann, U.S., Charles, C.D., and Hodell, D.A., 1999. Origin of global millennial-scale climate events: constraints from the southern ocean deep-sea sedimentary record. *In* Clark, P.U., Webb, R.S., and Keigwin, L.D. (Eds.), *Mechanisms of Global Climate Change at Millennial Time Scales.* Am. Geophys. Union, Monogr., 112:99–112.

Oppo, D.W., and Horowitz, M., 2000. Glacial deep water geometry: South Atlantic benthic foraminiferal Cd/Ca and ^{13}C evidence. *Paleoceanography,* 15:147–160.

Oppo, D.W., Keigwin, L.D., McManus, J.F., and Cullen, J.L., 2001. Persistent suborbital climate variability in marine isotope Stage 5 and Termination II. *Paleoceanography,* 16:280–292.

Peterson, L.C., and Prell, W.L., 1985. Carbonate preservation and rates of climatic change: an 800 kyr record from the Indian Ocean. *In* Sundquist, E.T., and Broecker, W.S. (Eds.), *The Carbon Cycle and Atmospheric CO_2: Natural Variations Archean to Present.* Geophys. Monogr., Am. Geophys. Union, 32:251–270.

Petit, J.R., Jouzel, J., Raynaud, D., Barkov, N.I., Barnola, J.-M., Basile, I., Bender, M., Chappellaz, J., Davis, M., Delaygue, G., Delmotte, M., Kotlyakov, M., Legrand, M., Lipenkov, Y., Lorius, C., Pepin, L., Ritz, C., Saltzman, E., and Stievenard, M., 1999. Climate and atmospheric history of the past 420,000 years from the Vostok ice core, Antarctica. *Nature*, 399:429–436.

Pichon, J.J., Labeyrie, L.D., Bareille, G., Labracherie, M., Duprat, J., and Jouzel, J., 1992. Surface water temperature changes in the high latitudes of the Southern Hemisphere over the last glacial–interglacial cycle. *Paleoceanography,* 7:289–318.

Porter, S.C., 2000. Onset of neoglaciation in the Southern Ocean. *J. Quat. Sci.,* 15:395–400.

Raymo, M.E., Hodell, D., and Jansen, E., 1992. Response of deep ocean circulation to initiation of Northern Hemisphere glaciation (3–2 Ma). *Paleoceanography,* 7:645–672.

Raymo, M.E., Ruddiman, W.F., Shackleton, N.J., and Oppo, D.W., 1990. Evolution of Atlantic-Pacific $\delta^{13}C$ gradients over the last 2.5 m.y. *Earth Planet. Sci. Lett.,* 97:353–368.

Robert, C., and Kennett, J.P., 1997. Antarctic continental weathering changes during Eocene–Oligocene cryosphere expansion: clay mineral and oxygen isotope evidence. *Geology,* 25:587–590.

Sachs, J.P., Anderson, R.F., and Lehman, S.J., 2001. Glacial surface temperatures of the southeast Atlantic Ocean. *Science*, 293:2077–2079.

Salamy, K.A., and Zachos, J.C., 1999. Latest Eocene–early Oligocene climate change and Southern Ocean fertility: inferences from sediment accumulation and stable isotope data. *Palaeogeogr., Palaeoclimatol., Palaeoecol.,* 145:61–77.

Shackleton, N.J., 2000. The 100,000-year ice-age cycle identified and found to lag temperature, carbon dioxide, and orbital eccentricity. *Science*, 289:1897–1902.

Shackleton, N.J., Crowhurst, S.J., Weedon, G.P., and Laskar, J., 1999. Astronomical calibration of Oligocene–Miocene time. *Philos. Trans. R. Soc. London, Ser. A,* 357:1907–1929.

Shackleton, N.J., Hall, M.A., and Pate, D., 1995. Pliocene stable isotope stratigraphy of Site 846. *In* Pisias, N.G., Mayer, L.A., Janecek, T.R., Palmer-Julson, A., and van Andel, T.H. (Eds.), *Proc. ODP, Sci. Results,* 138: College Station, TX (Ocean Drilling Program), 337–355.

Shackleton, N.J., Hall, M.A., Raffi, I., Tauxe, L., and Zachos, J., 2000. Astronomical calibration age for the Oligocene–Miocene boundary. *Geology,* 28:447–450.

Shemesh, A., Hodell, D.A., Crosta, X., Kanfoush, S.K., Charles, C.D., and Guilderson, T.P., 2002. The sequence of events during the last deglaciation in Southern Ocean sediments and Antarctic ice cores. *Paleoceanography*, 10.1029/2000PA000599.

Shipboard Scientific Party, 1999. Leg 177 summary: Southern Ocean paleoceanography. *In* Gersonde, R., Hodell, D.A., Blum, P., et al., *Proc. ODP, Init. Repts.,* 177: College Station, TX (Ocean Drilling Program), 1–67.

————, 2001. Leg 189 summary. *In* Exon, N.F., Kennett, J.P., Malone, M.J., et al., *Proc. ODP, Init. Repts.,* 189: College Station TX (Ocean Drilling Program), 1–98.

Sigman, D.M., and Boyle, E.A., 2000. Glacial/interglacial variations in atmospheric carbon dioxide. *Nature,* 407:859–869.

Smith, D.G., Ledbetter, M.T., and Ciesielski, P.F., 1983. Ice-rafted volcanic ash in the South Atlantic sector of the Southern Ocean during the last 100,000 years. *Mar. Geol.,* 53:291–312

Spero, H.J., and Lea, D.W., 2002. The cause of carbon isotope minimum events on glacial terminations. *Science,* 296:522–525.

Stephens, B.B., and Keeling, R.F., 2000. The influence of Antarctic sea ice on glacial-interglacial CO_2 variation. *Nature,* 404:171–174.

Stoner, J.S., Channell, J.E.T., Hodell, D.A., and Charles, C.D., in press. A ~570-kyr geomagnetic paleosecular variation record from the sub-Antarctic South Atlantic (ODP Site 1089). *J. Geophys. Res.*

Stoner, J.S., Laj, C., Channell, J.E.T., and Kissel, C., 2002. South Atlantic and North Atlantic geomagnetic paleointensity stacks (0–80 ka): implications for inter-hemispheric correlation. *Quat. Sci. Rev.*, 21:1141–1151.

Toggweiler, J.R., 1999. Variation of atmospheric CO_2 by ventilation of the ocean's deepest water. *Paleoceanography,* 14:571–588.

Venz, K.A., and Hodell, D.A., 2002. New evidence for changes in Plio–Pleistocene deep water circulation from Southern Ocean ODP Leg 177 Site 1090. *Palaeogeogr., Palaeoclimatol., Palaeoecol.,* 182:197–220.

Warnke, D.A., Allen, C.P., Müller, D.W., Hodell, D.A., and Brunner, C., 1992. Miocene–Pliocene Antarctic glacial evolution: a synthesis of ice-rafted debris, stable isotope, and planktonic foraminiferal indicators, ODP Leg 114. *In* Kennett, J.P., and Warnke, D.A. (Eds.), *The Antarctic Paleoenvironment: A Perspective on Global Change*. Am. Geophys. Union, Antarct. Res. Ser., 56:311–325.

Wildeboer Shut, E., Uenzelmann-Neben, G., and Gersonde, R., 2002. Seismic evidence for bottom current activity at the Agulhas Ridge. *Global and Planet. Change,* 34:185–198.

Yokoyama, Y., Esat, T.M., and Lambeck, K., 2001. Coupled climate and sea-level changes deduced from Huon Peninsula coral terraces of the last ice age. *Earth Planet. Sci. Lett.,* 193:579–587.

Zachos, J.C., Breza, J.R., and Wise, S.W., 1992. Early Oligocene ice-sheet expansion on Antarctica: stable isotope and sedimentological evidence from Kerguelen Plateau, southern Indian Ocean. *Geology,* 20:569–573.

Zachos, J.C., Pagani, M., Sloan, L., Thomas, E. and Billups, K., 2001a. Trends, rhythms, and aberrations in global climate 65 Ma to present. *Science,* 292:686–693.

Zachos, J.C., Quinn, R.M., and Salamy, K., 1996. High resolution (10^4 yr) deep-sea foraminiferal stable isotope records of the Eocene–Oligocene climate transition. *Paleoceanography,* 11:251–266.

Zachos, J.C., Shackleton, N.J., Revenaugh, J.S., Pälike, H., and Flower, B.P., 2001b. Climate response to orbital forcing across the Oligocene–Miocene boundary. *Science,* 292:274–278.

Zielinski, U., Bianchi, C., Gersonde, R., and Kunz-Pirrung, M., 2002. Last occurrence datums of the diatoms *Rouxia leventerae* and *R. constricta*—indicators for marine isotope stages 6 and 8 in Southern Ocean sediments. *Mar. Micropaleontol.,* 46:127–137.

Zielinski, U., and Gersonde, R., 2002. Plio–Pleistocene diatom biostratigraphy from ODP Leg 177, Atlantic sector of the Southern Ocean. *Mar. Micropaleontol.,* 45:225–268.

Figure F1. Seven sites oriented along a north-south transect from 41° to 54°S were drilled during Leg 177, crossing each of the major fronts of the Antarctic Circumpolar Current.

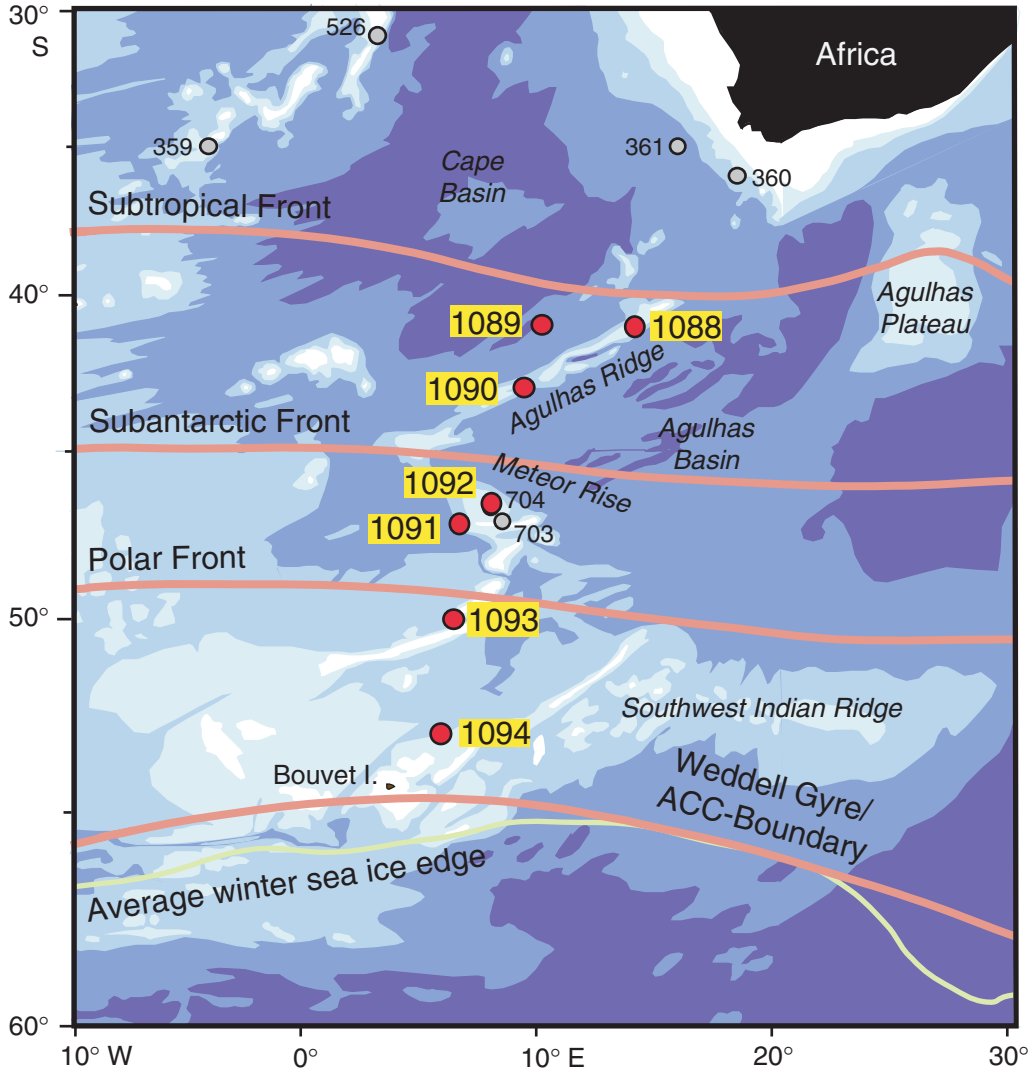

Figure F2. A. Vertical distribution of $\delta^{13}C$ of dissolved inorganic carbon (Kroopnick, 1985) in the world's oceans (after Charles and Fairbanks, 1992). **B.** Positions of Leg 177 sites relative to the distribution of $\delta^{13}C$ in the South Atlantic Ocean. Several Leg 177 studies have used benthic $\delta^{13}C$ to reconstruct changes in deep-water circulation. Note the tongue of NADW with high $\delta^{13}C$ values as it penetrates into the South Atlantic and inserts itself into Antarctic circumpolar flow. CDW = Circumpolar Deep Water, NADW = North Atlantic Deep Water (after Ninnemann and Charles, 2002).

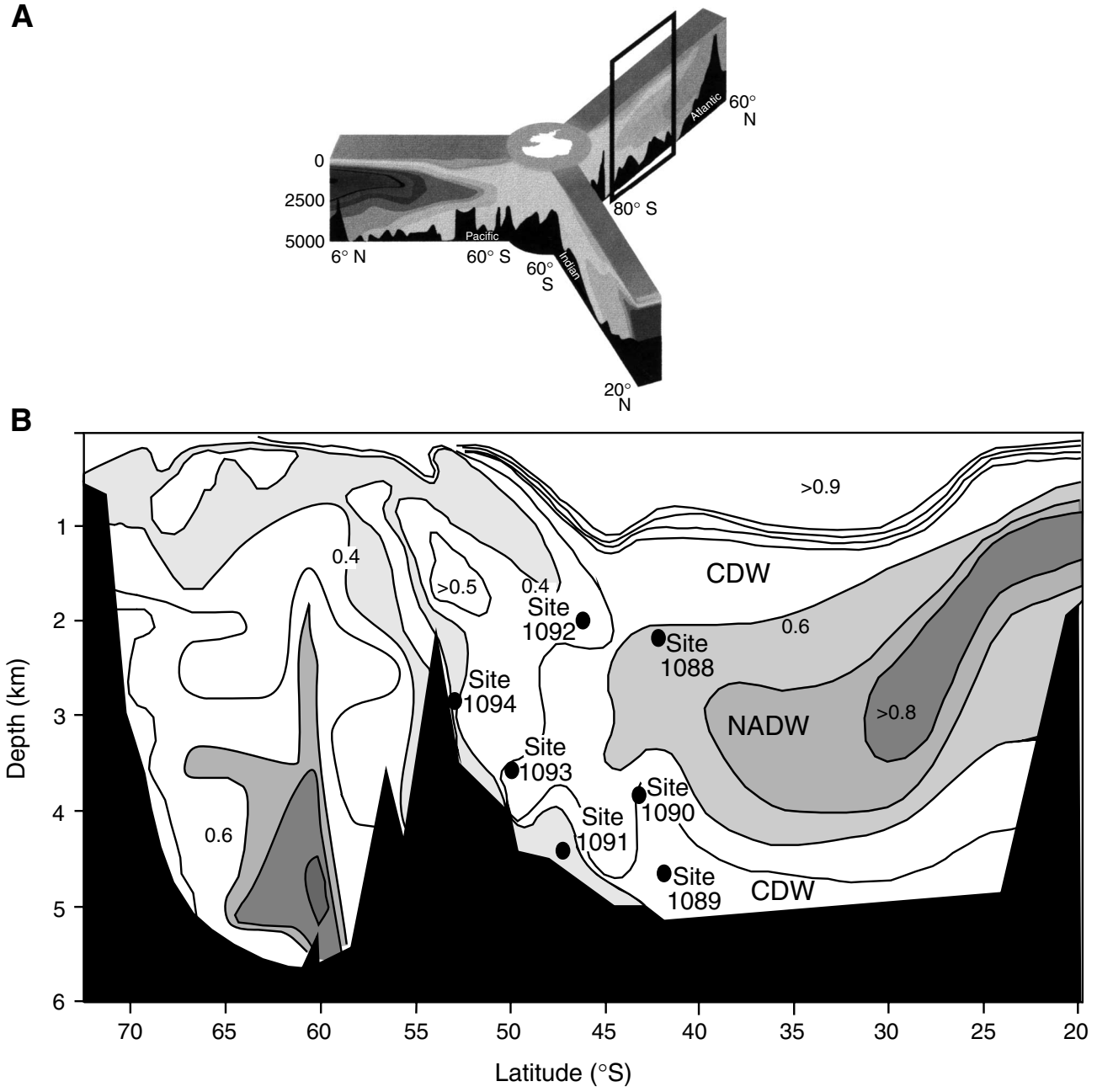

Figure F3. Correlation of oxygen isotope and color reflectance records at Sites 1089 (41°S), 1093 (50°S), and 1094 (53°S). Marine isotope stages represent the major terminations of the late Pleistocene. The great depth of these stage boundaries illustrates the high sedimentation rates, especially at Site 1093. The oxygen isotope record at the lowest-latitude Site 1089 is nearly complete, but the signals at higher-latitude Sites 1093 and 1094 are discontinuous because of the scarcity of foraminifers (Hodell et al., **Chap. 9,** this volume).

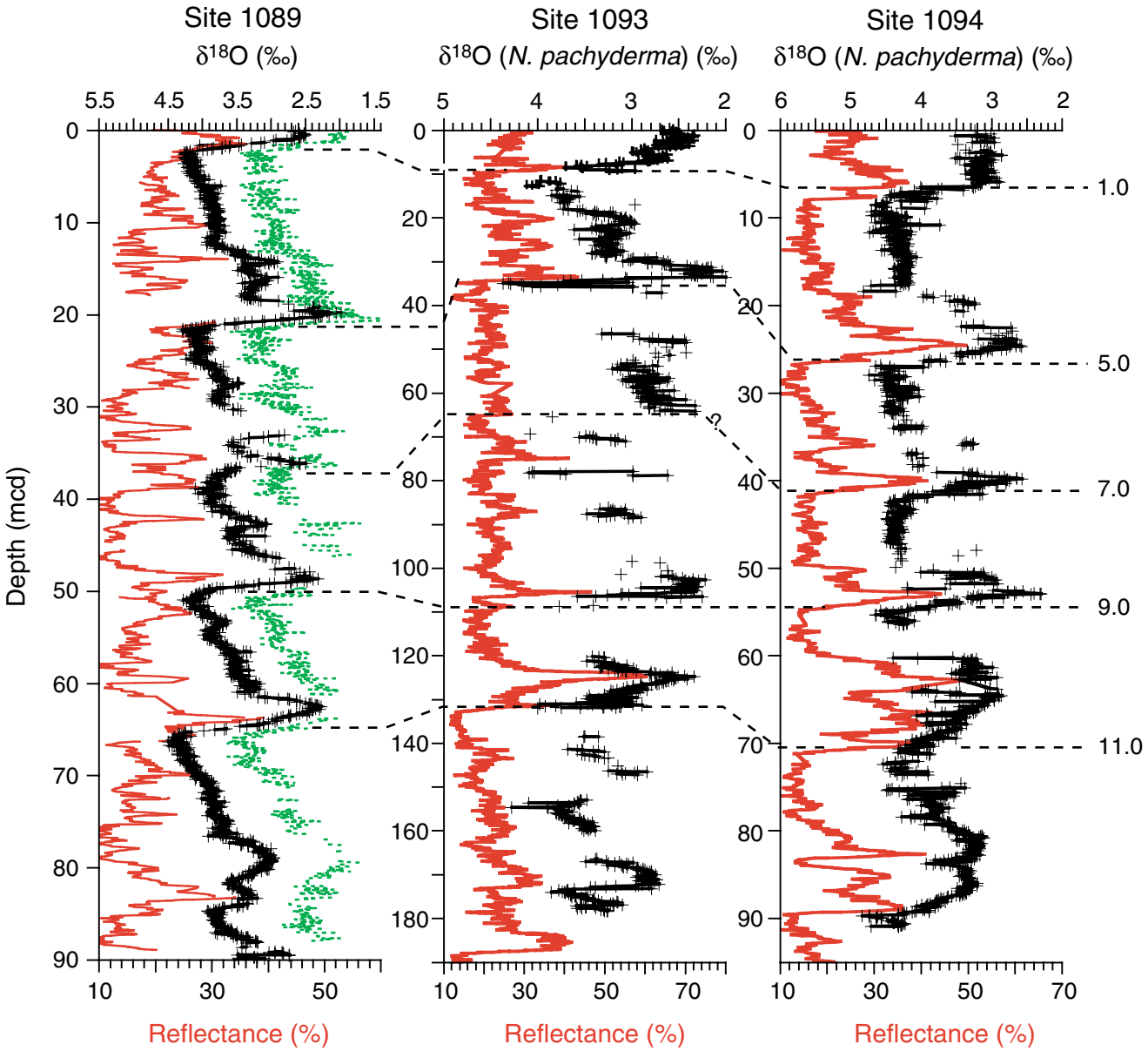

Figure F4. Correlation of benthic $\delta^{18}O$ records at Sites 1088, 1090, and 1092 with the reference signal from Site 607. Although these sites have lower sedimentation rates than the high-resolution ones (Sites 1089, 1093, and 1094), nearly all oxygen isotope stages are identifiable for the Pliocene–Pleistocene (Hodell et al., Chap. 9, this volume; Andersson et al., 2002).

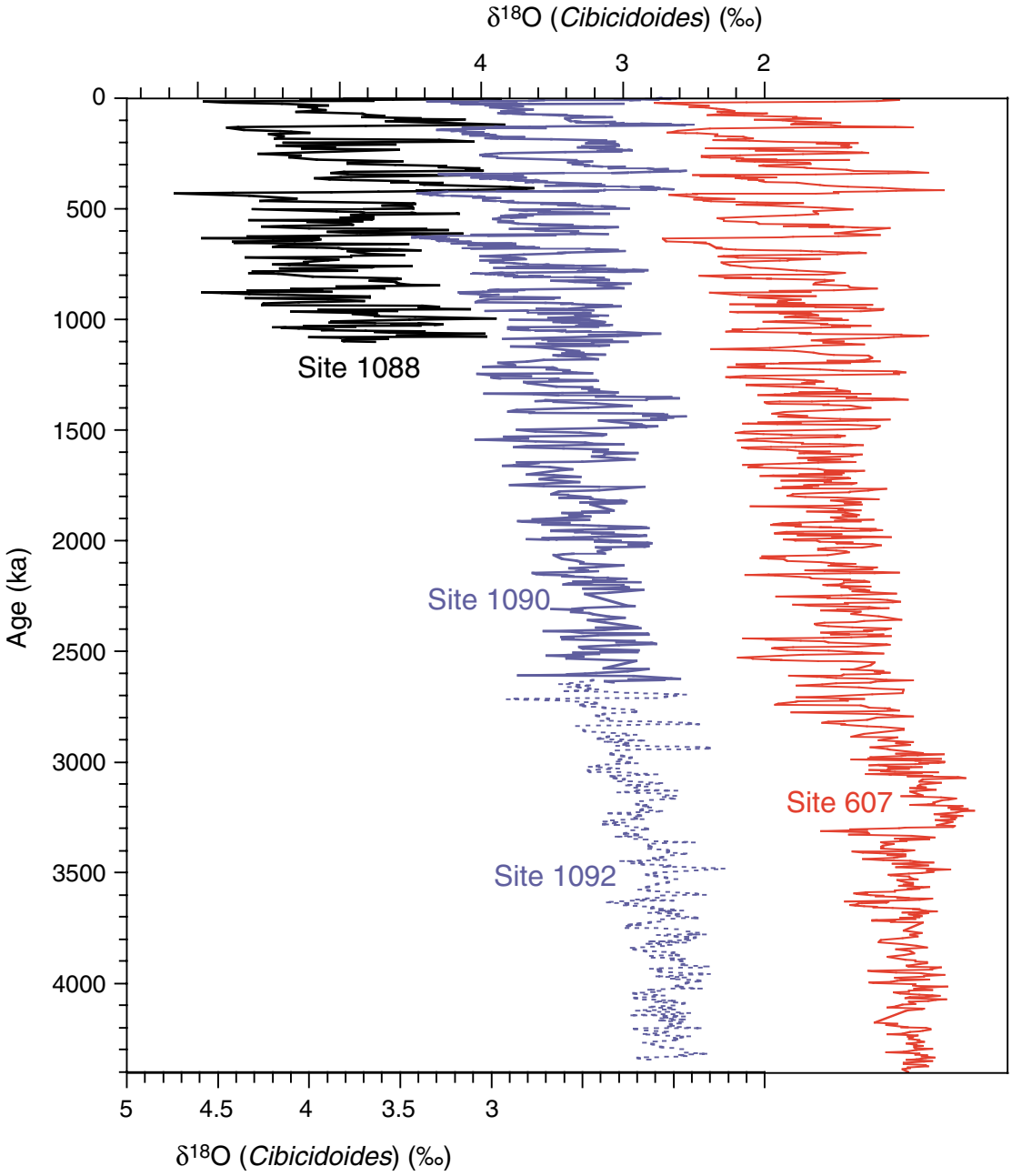

Figure F5. Correlation of benthic $\delta^{18}O$ signal at Site 1090 in the late Oligocene and early Miocene with the astronomically tuned $\delta^{18}O$ record from Site 929 on the Ceara Rise (after Billups et al., 2002). This correlation can be used to directly relate the astronomically tuned Site 929 chronology to the polarity reversal stratigraphy at Site 1090 (Channell et al., in press). CM–O/M = carbon isotope maximum at the Oligocene/Miocene boundary (Hodell and Woodruff, 1994). Mi 1 and Mi 1a represent Miocene glacial events (Miller et al., 1991).

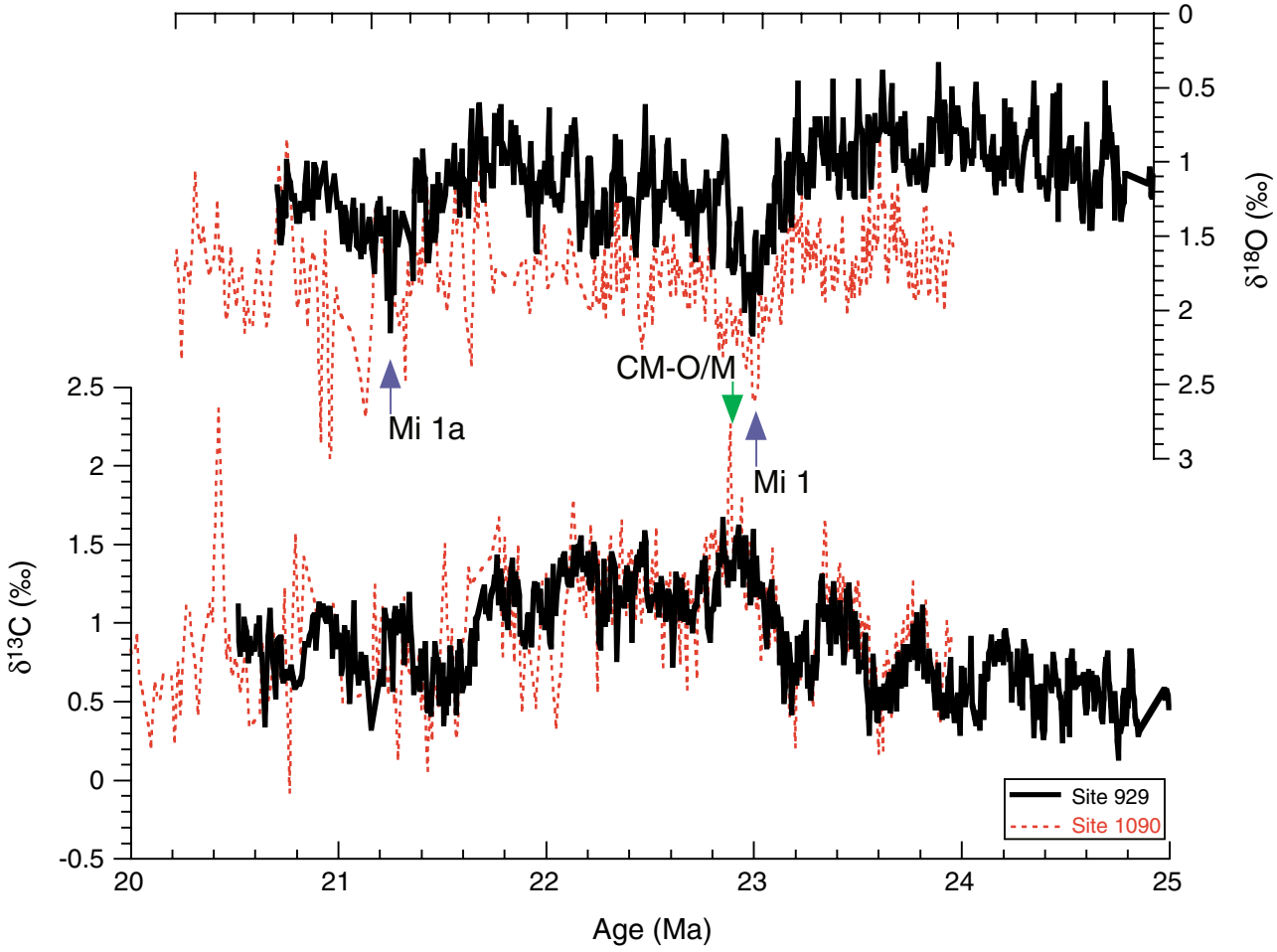

Figure F6. Correlation of geomagnetic paleointensity records from Site 1089 and site-survey piston cores from the sub-Antarctic South Atlantic. The similarly of these records demonstrated that a consistent signal was recorded despite differences in sediment lithology and accumulation rates (after Stoner et al., 2002).

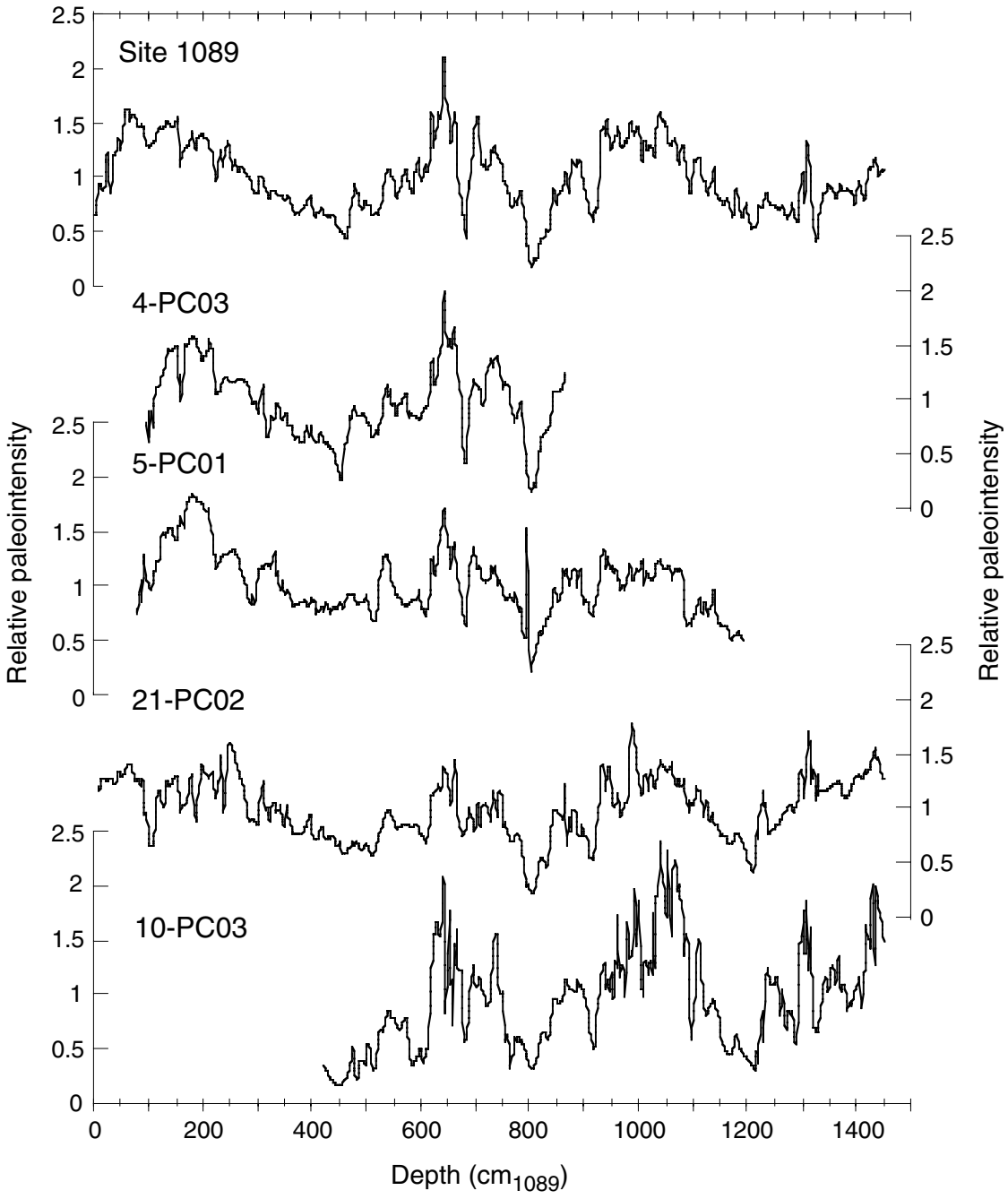

Figure F7. A. Correlation of oxygen isotope records at Site 1089 [b; black line] and Site 983 [c; green line] with the SPECMAP $\delta^{18}O$ reference curve [a; red line]. **B.** Correlation of geomagnetic paleointensity record at Site 1089 [e; black line] with Site 983 [f; green line] and the composite Sint-800 record (Guyodo and Valet, 1999) [d; red line] (after Stoner et al., in press).

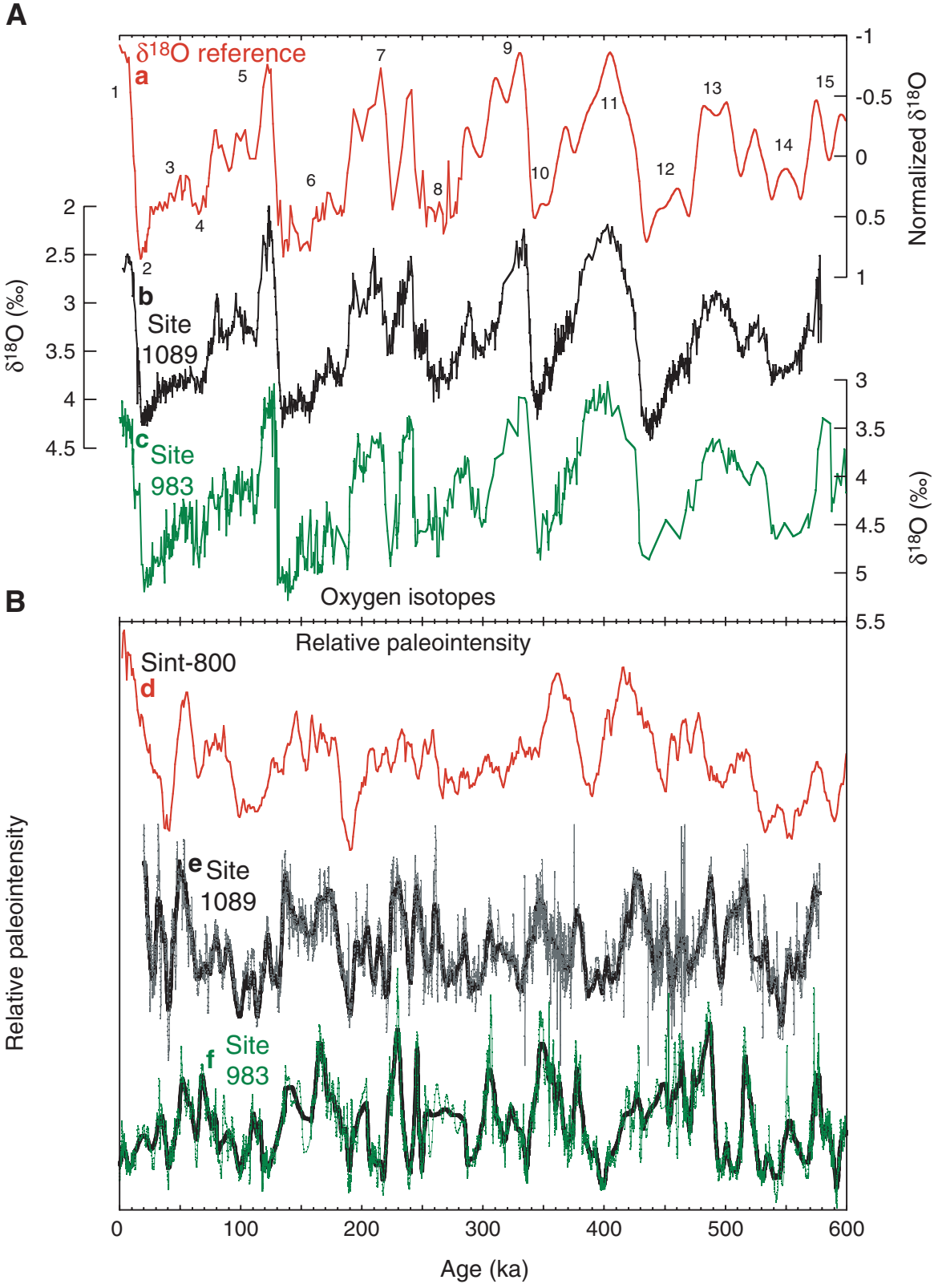

Figure F8. Composite benthic $\delta^{18}O$ record illustrating the major climatic events of the Cenozoic (modified after Zachos et al., 2001a). Also shown is the time span of selected Leg 177 postcruise studies and some of the major events in Southern Ocean paleoceanographic evolution inferred from these studies. NADW = North Atlantic Deep Water, S.O. = Southern Ocean, SOW = Southern Ocean Water, ACC = Antarctic Circumpolar Current. * = the $\delta^{18}O$ temperature scale was calculated for an ice-free world and thus applies only to the time period older than ~35 Ma.

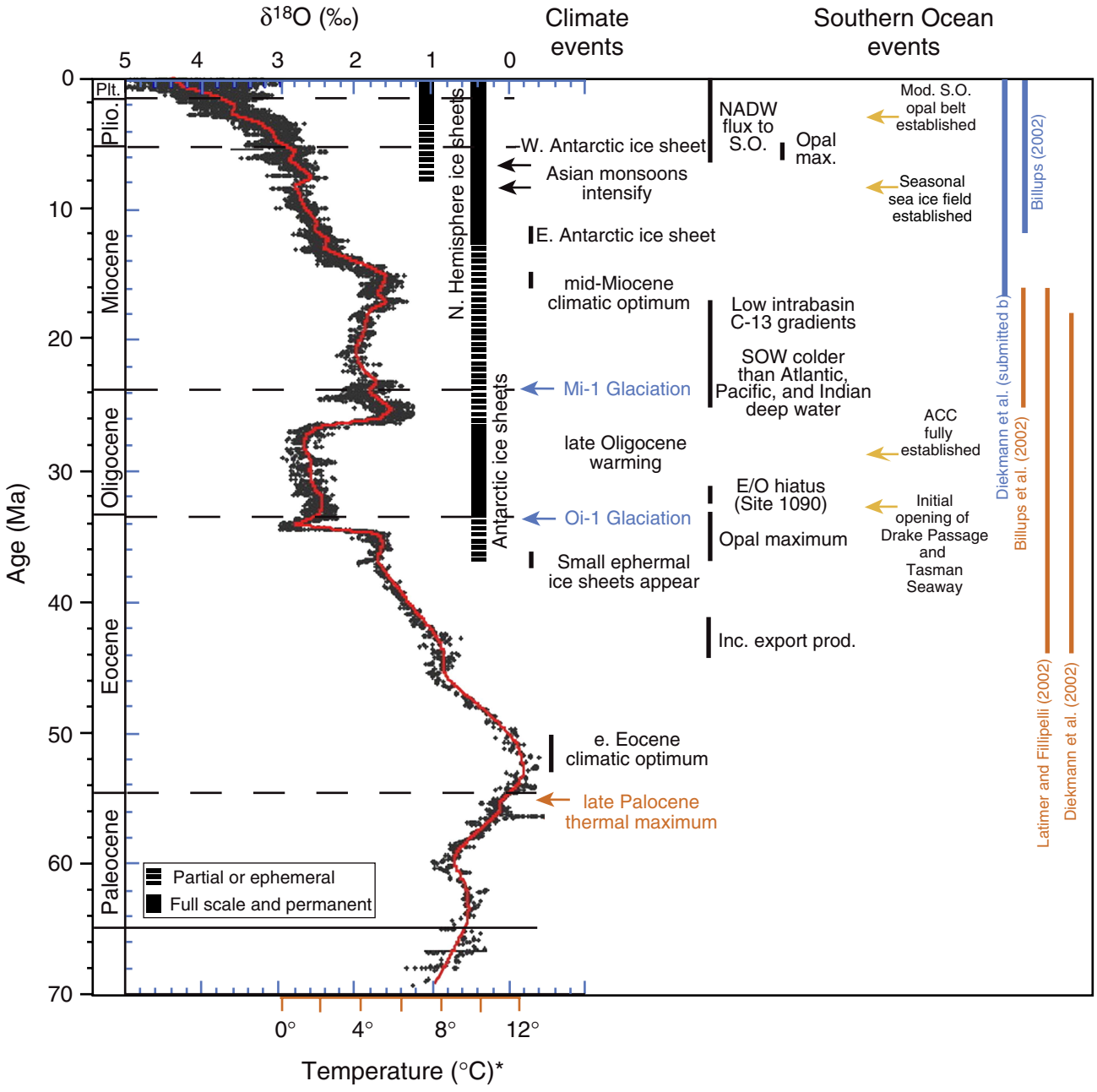

Figure F9. Seven-point smoothed elemental ratios and total Ba concentrations at Site 1090 showing an important change in terrigenous and biogenous sedimentation across the Eocene/Oligocene boundary that were interpreted to be related to the opening of the Drake Passage (after Latimer and Filippelli, 2002). **A.** Al/Ti. **B.** P/Al. **C.** Ba/Al. **D.** Ba.

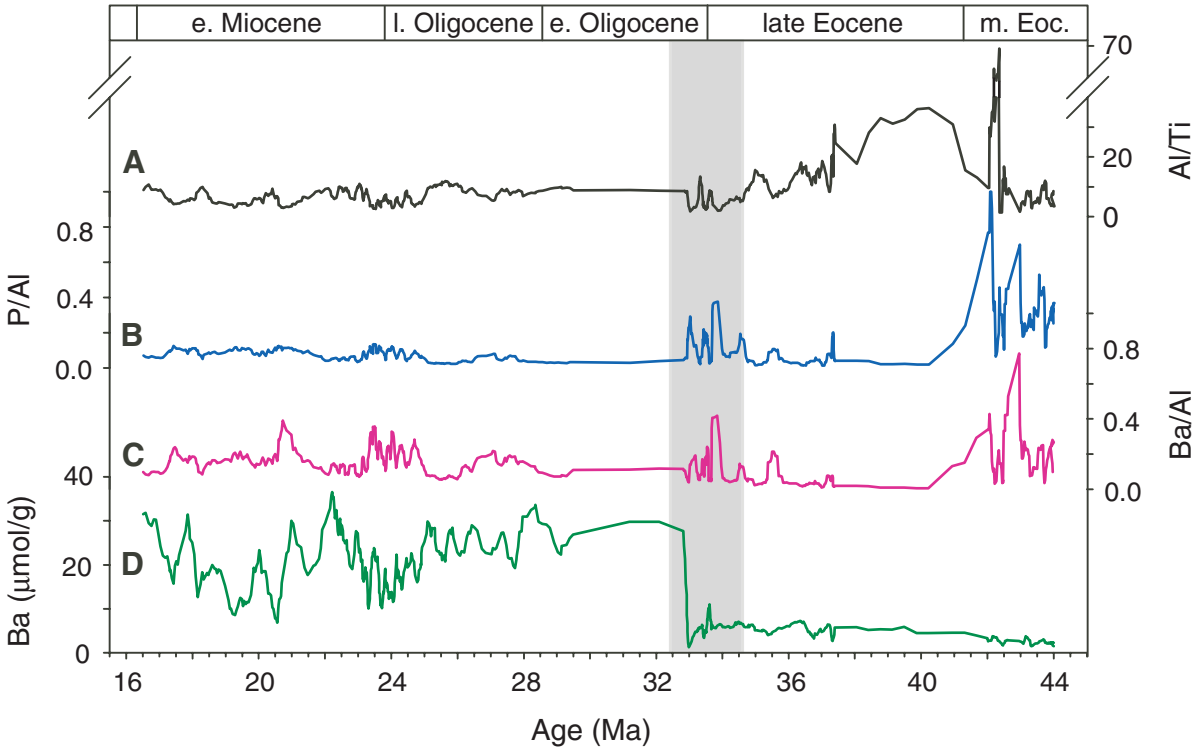

Figure F10. A. Comparison of benthic $\delta^{18}O$ records among Sites 1092 (blue dashed line), 704 (red line), and 849 (black line). Note that Southern Ocean Sites 1092 and 704 have significantly higher $\delta^{18}O$ values than Pacific Site 849. **B.** Comparison of benthic $\delta^{13}C$ signals from the North Atlantic Site 607 (red line) and Site 925 (magenta line), Southern Ocean Site 1092 (blue dashed line), and Pacific Site 849 (black line) (after Andersson et al., 2002).

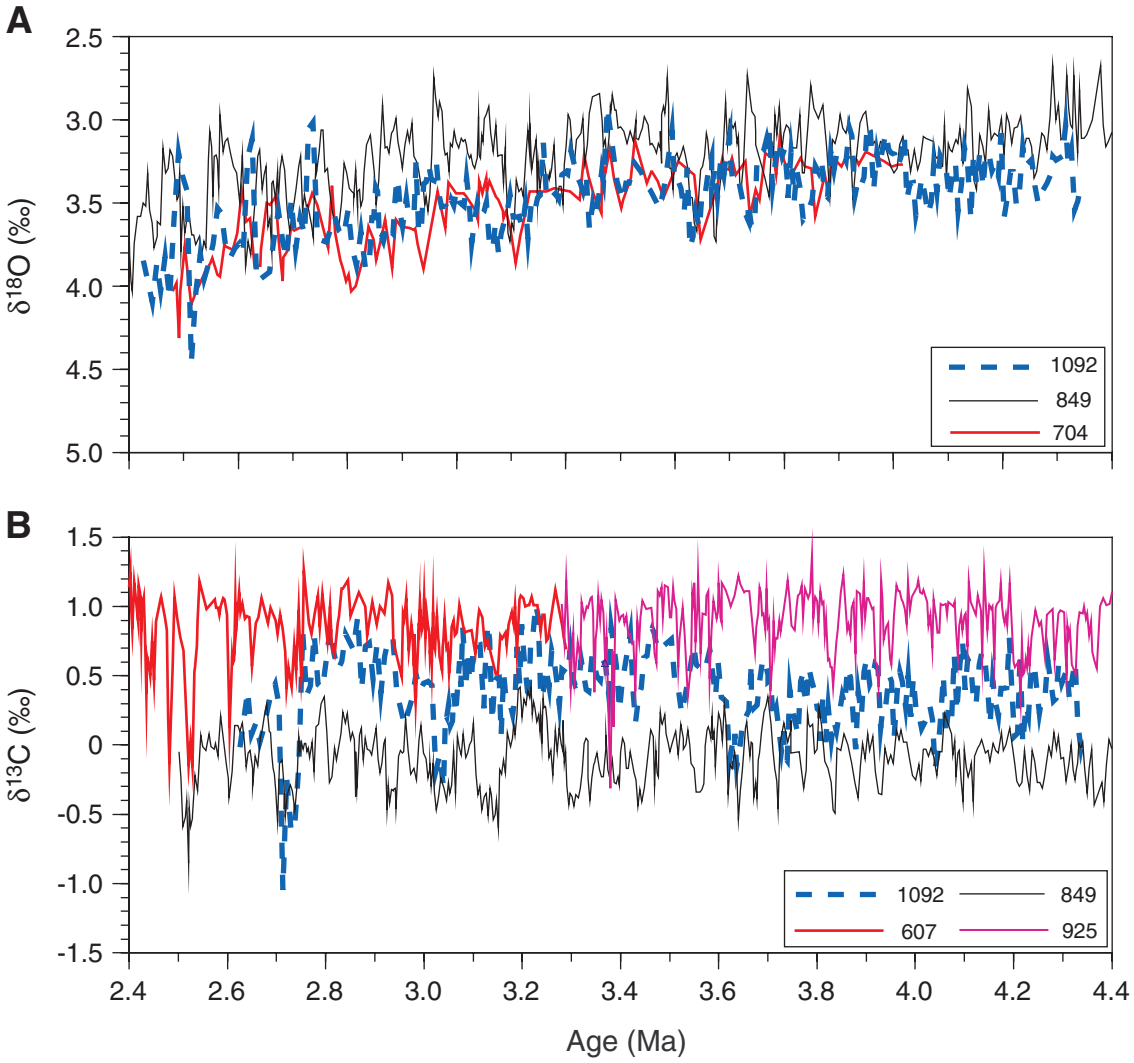

Figure F11. Comparison of benthic $\delta^{13}C$ signals between the deep Pacific Site 849 (blue dashed line) (Mix et al., 1995), Southern Ocean Site 1090 (red line, solid circles) (Venz and Hodell, 2002) and Site 1092 (red line, open circles) (Andersson et al., 2002) and North Atlantic Site 607 (black line) (Raymo et al., 1990, 1992). Note that Southern Ocean benthic $\delta^{13}C$ values decreased in two pronounced steps at 2.75 and 1.55 Ma relative to records in the North Atlantic and Pacific Oceans. At 2.75 Ma, Southern Ocean $\delta^{13}C$ values shift away from the North Atlantic and overlap those in the Pacific. After 1.55 Ma, Southern Ocean $\delta^{13}C$ values were consistently lower than those in the Pacific during glacial periods.

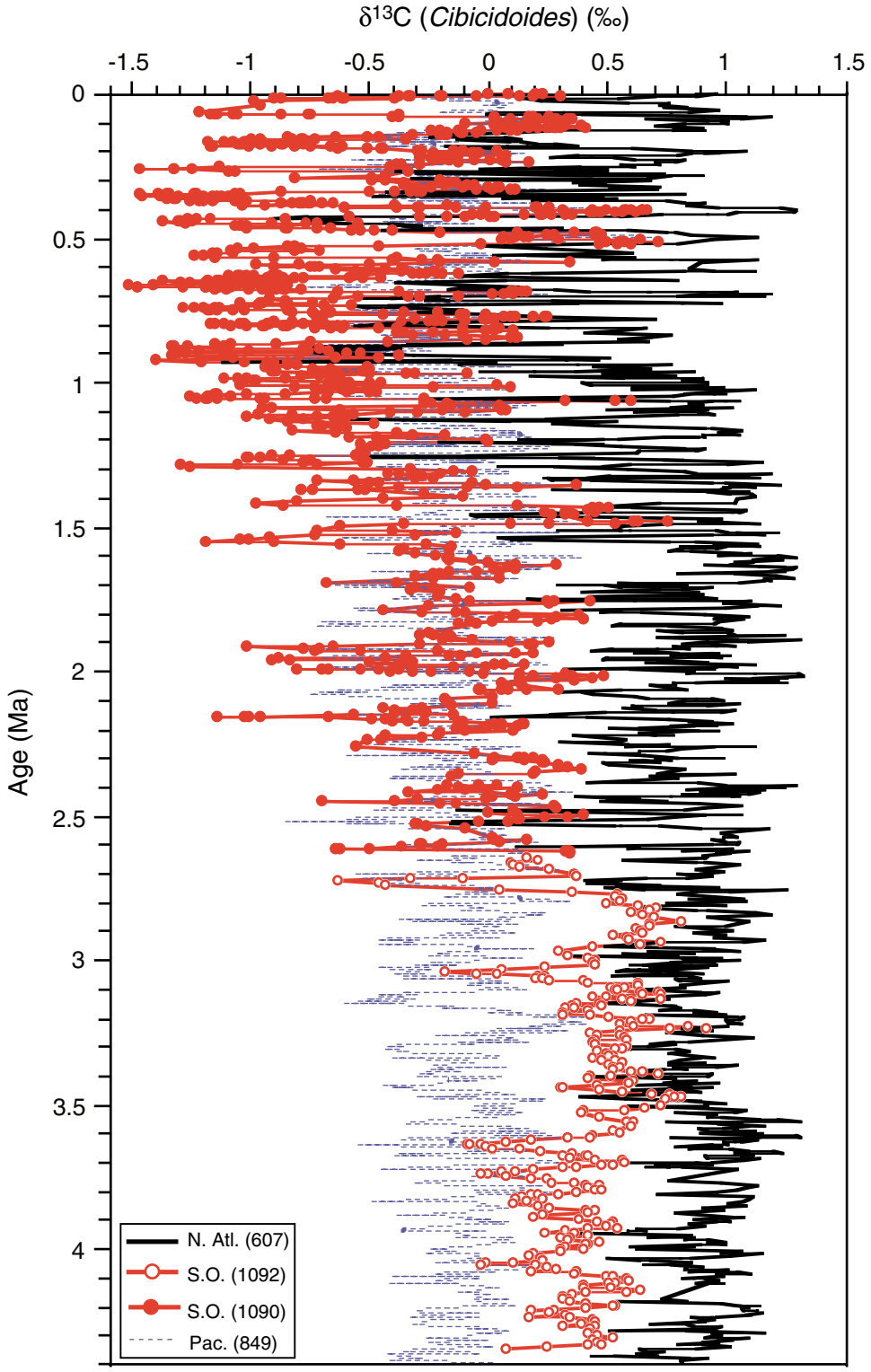

Figure F12. Composite Southern Ocean benthic $\delta^{18}O$ record for the Pliocene–Pleistocene produced by combining data from Site 1090 (2.6–0 Ma) (Venz and Hodell, 2002) and Site 1092 (2.6–4.4 Ma) (Andersson et al., 2002). Shown are some of the major climatic and paleoceanographic events inferred from Leg 177 and other studies. IRD = ice-rafted debris, MBT = mid-Brunhes Transition, MPT = mid-Pleistocene Transition, S.O. = Southern Ocean, SSST = summer sea-surface temperature, PFZ = Polar Front Zone, eMDM = early Matumaya Diatom Maximum, lMDM = late Matumaya Diatom Maximum.

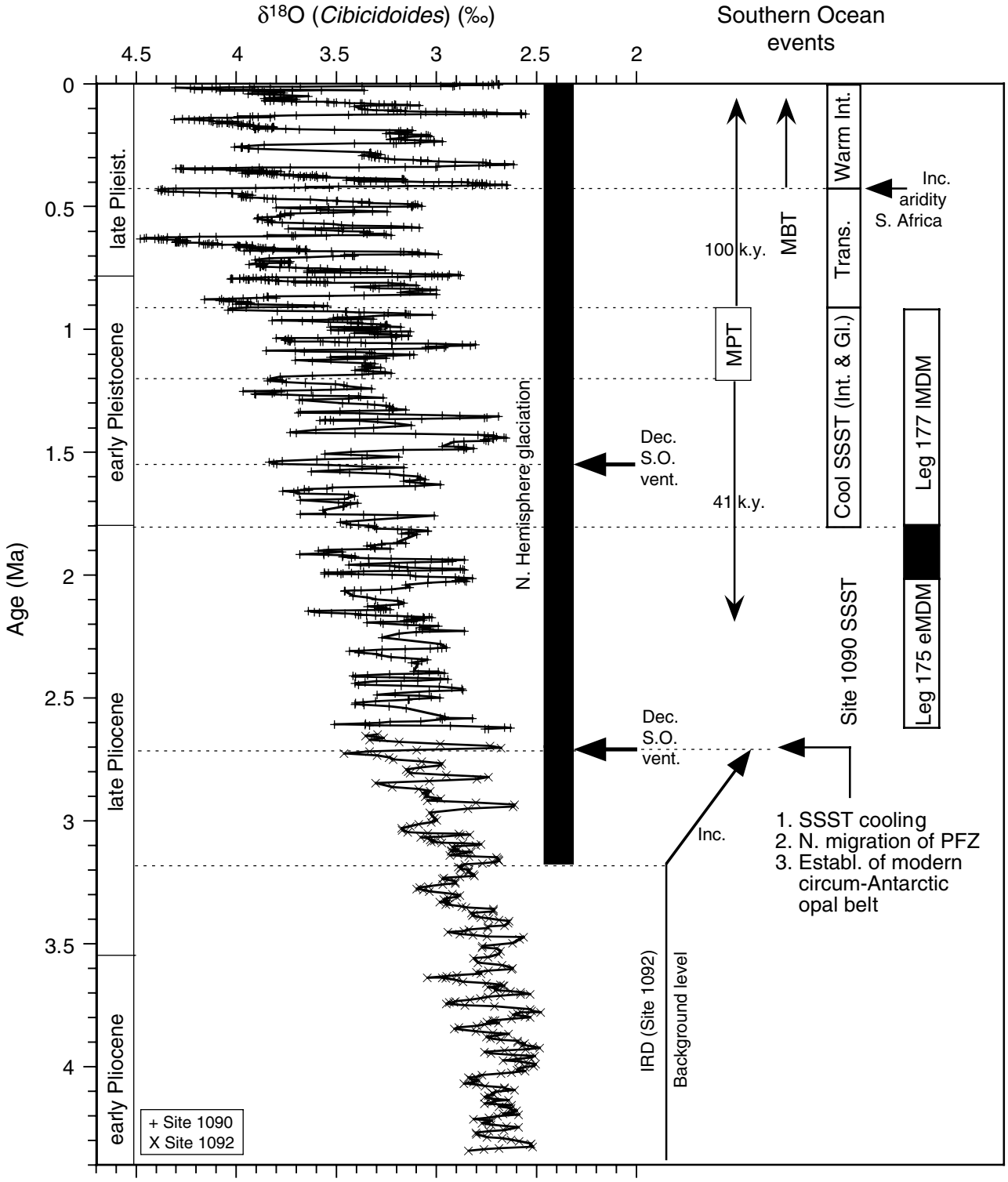

Figure F13. Pleistocene summer sea-surface temperature (SSST) record obtained at subantarctic Site 1090 (after Becquey and Gersonde, 2002, in press). Benthic foraminiferal $\delta^{18}O$ signal represents a composite constructed from core PS2489-2 and Site 1090. Variations in SSST (dark/blue line) and its standard deviation (light gray lines) were estimated using a planktonic foraminiferal transfer function. Vertical colored areas indicate modern temperature ranges at the Polar Front (PF), the Subantarctic Front (SAF), and the Subtropical Front (STF). Modern SSST at the core location is 10.2°C (Levitus and Boyer, 1994). MBE = Mid-Brunhes Event, B/M = Brunhes/Matuyama boundary (according to Shipboard Scientific Party, 1999), MPR = mid-Pleistocene Revolution. Age model according to Venz and Hodell (2002). MIS = marine isotope stage.

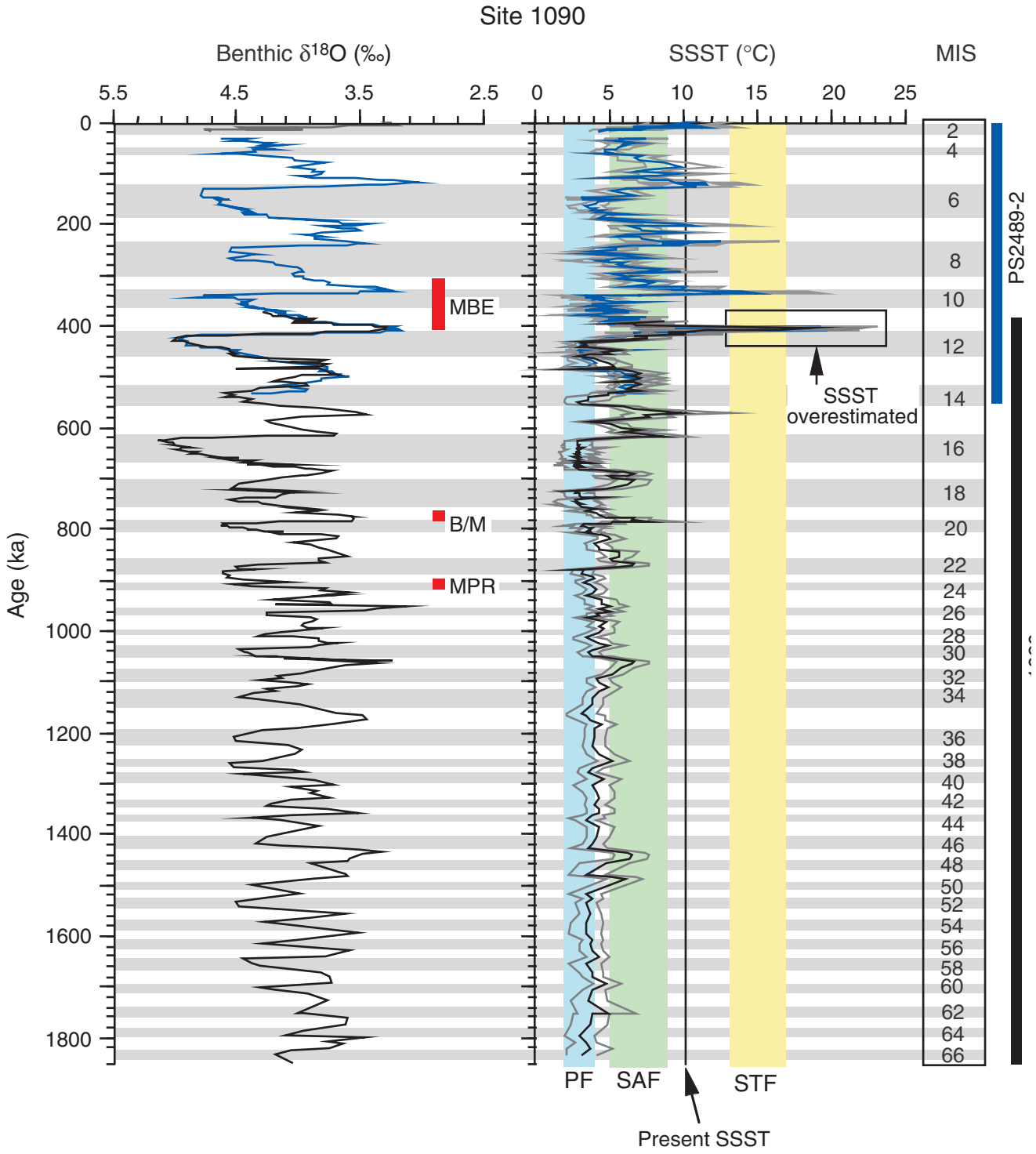

Figure F14. **A.** $\delta^{18}O$ of the planktonic foraminifer *G. bulloides* (Ninnemann et al., 1999; Mortyn et al., submitted [N5]) at ODP Site 1089. **B.** Radiolarian-based summer sea-surface temperature (SSST) record for PS2821/ODP Site 1089 (Cortese and Abelmann, 2002). **C.** Atmospheric paleotemperatures at the inversion layer reconstructed from the Vostok ice core (Antarctica), given as a difference from today's value (Petit et al., 1999). **D.** Blow-up of Figures **F14B–F14C**, p. 34, for a 30-k.y. interval including Termination I. The cooling events recognized in the SSST record of PS2821 during Termination I are labeled as YD (Younger Dryas)-I and ACR (Antarctic Cold Reversal)-I. For the Vostok ice core, the position of the ACR and an event similar to YD-I are also shown. **E.** Same as above, for Termination II. The positions of the cooling events recognized at this Termination in the SSST record of Site 1089 are labeled as YD-II and ACR-II (after Cortese and Abelmann, 2002).

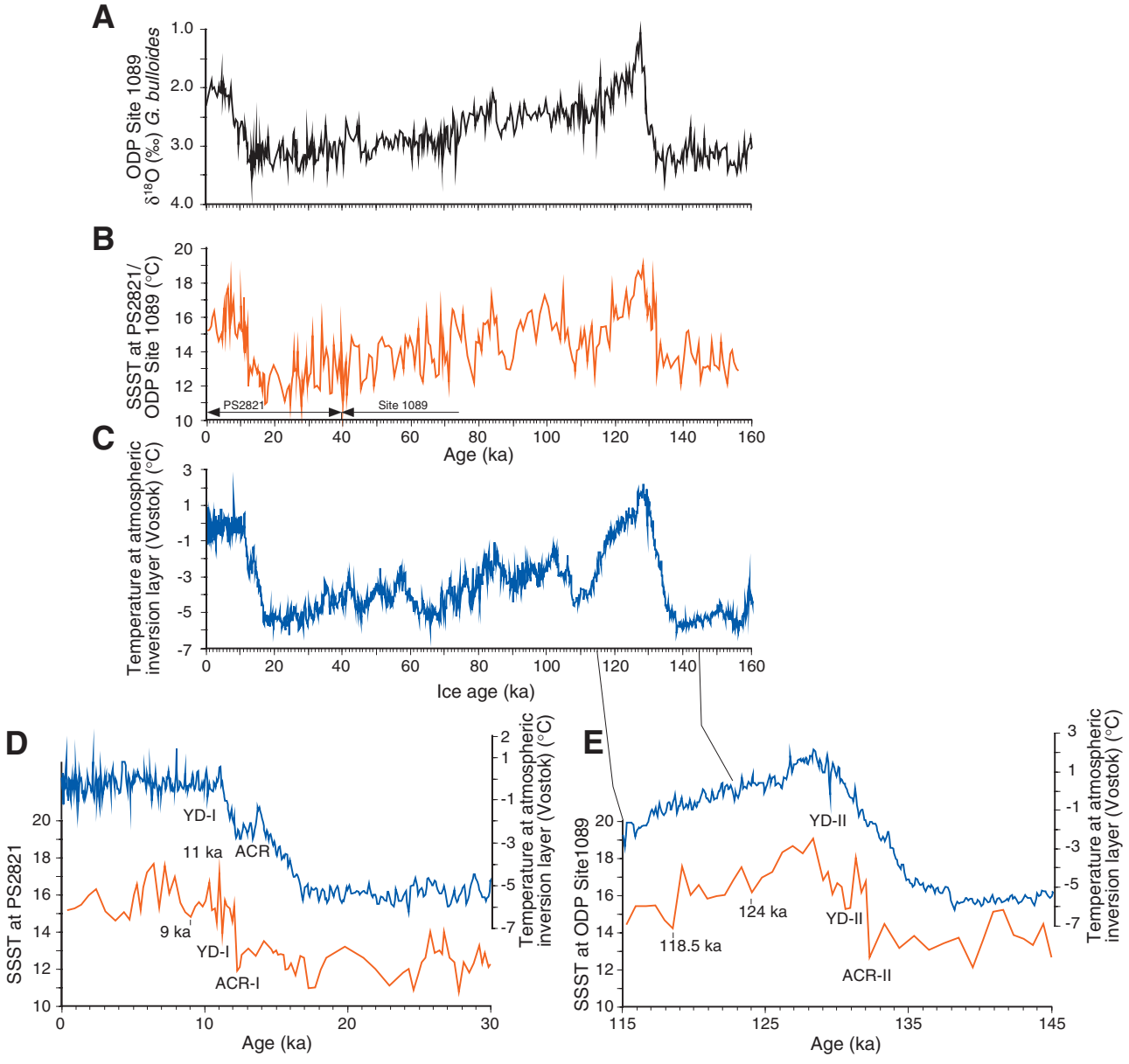

Figure F15. Comparison of diatom-based summer sea-surface temperature (SSST) at Sites 1093 and 1094 with atmospheric temperature at the inversion level (ΔT_i) of the Vostok ice core (Petit et al., 1999). The 4°C isotherm and Polar Front was displaced about 3° to the south during the climatic optimum of MIS 11 relative to today. The star indicates the fixed tie point at 390 ka (MIS 11.24) that is used in the age model for the Vostok ice core record (Petit et al., 1999). MIS = marine isotope stage (after Kunz-Pirrung et al., 2002).

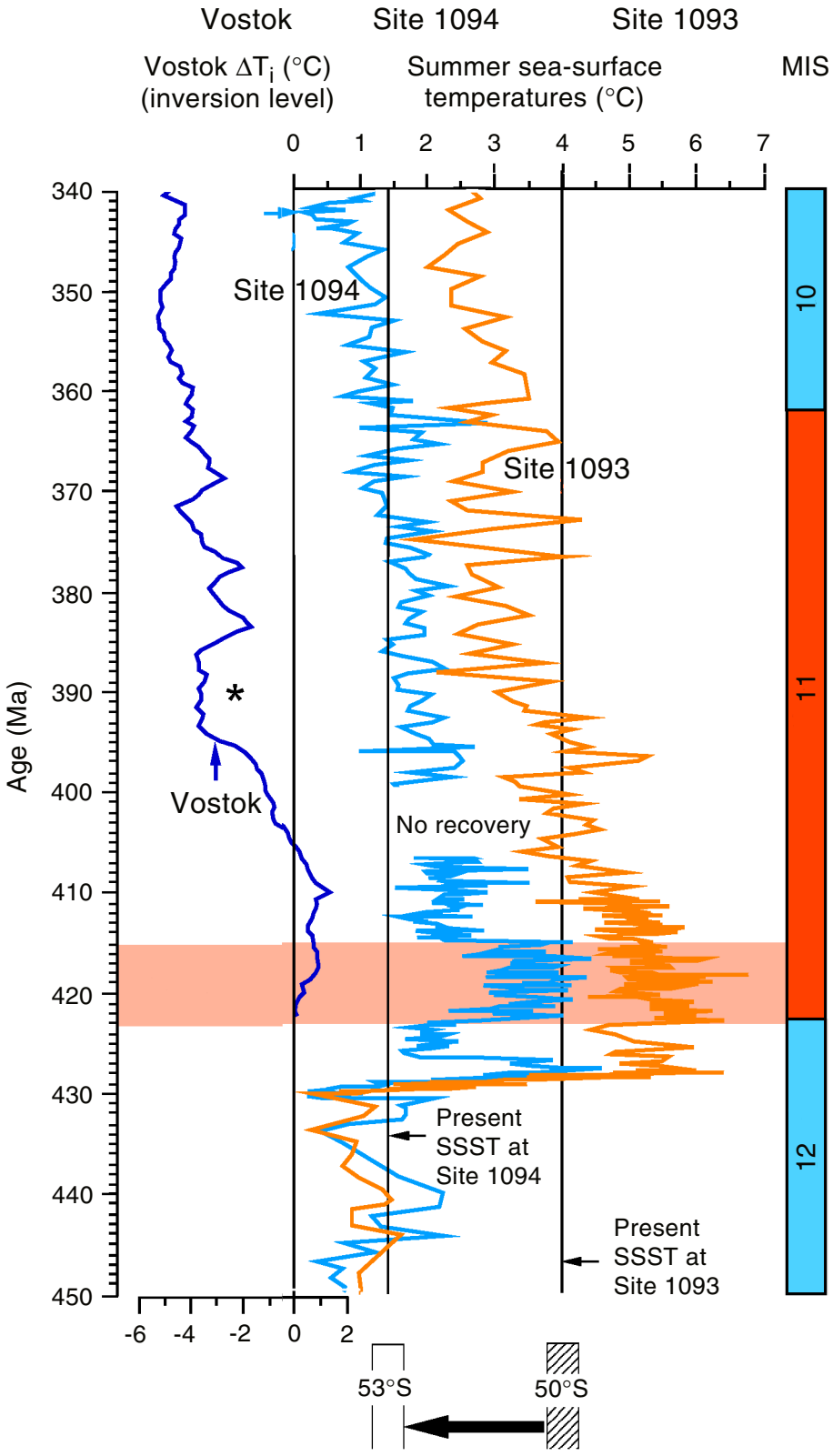

Figure F16. A. Correlation of percent ash (blue line) in the marine sediment record from Site 1094 and sodium concentration (dashed red line) in the Vostok ice core. **B.** Resulting comparison of $\delta^{18}O$ of *N. pachyderma* (green line), inferred temperatures from the Vostok ice core (dashed magenta line) (Petit et al., 1999), and lithic concentration at Site 1094 (black line) (after Kanfoush et al., 2002).

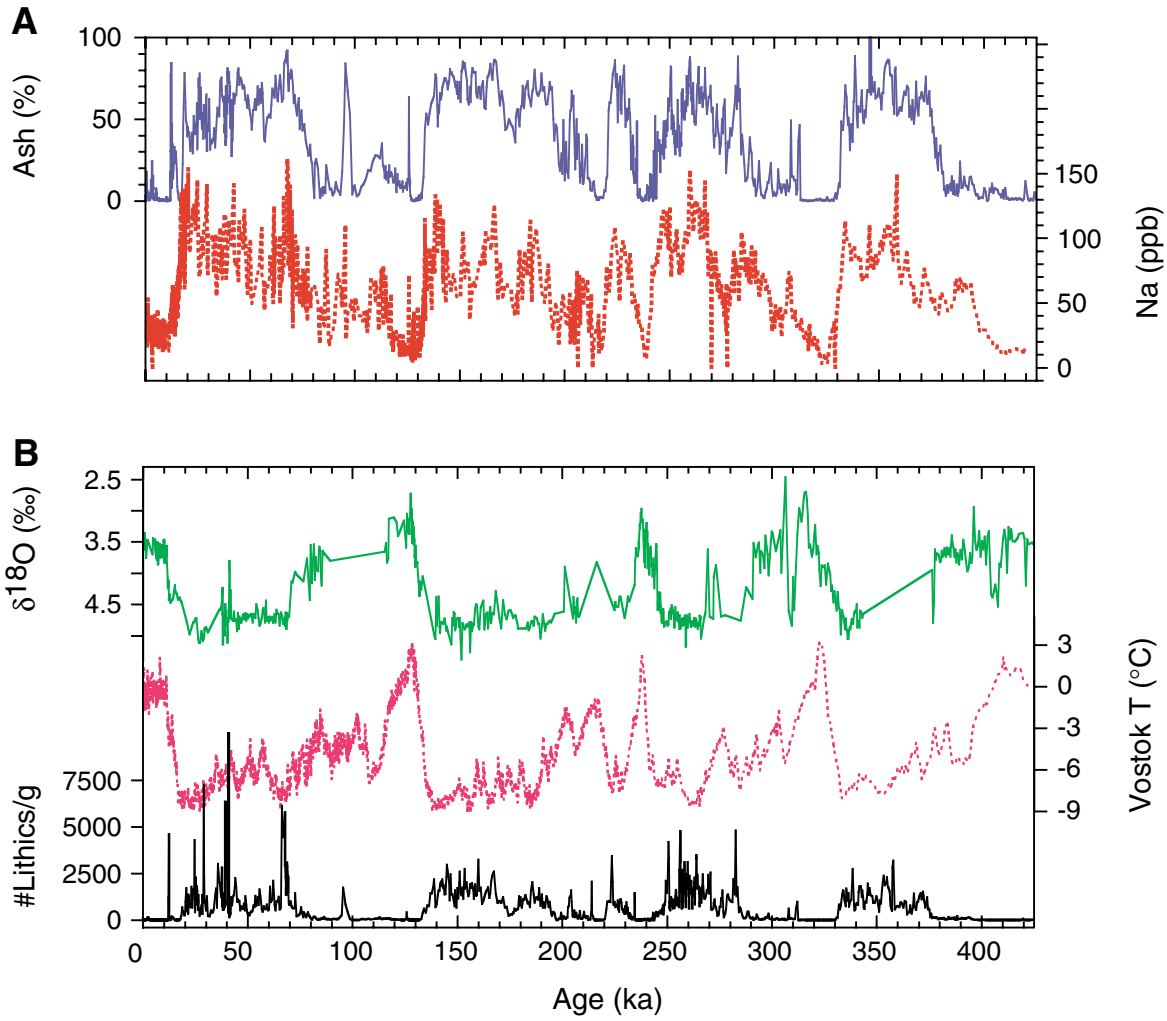

Figure F17. Contoured benthic $\delta^{13}C$ vs. time and water depth based on analysis of Sites 1088 (2082 m), 1090 (3702 m), and 1089 (4621 m). Note the sharp vertical $\delta^{13}C$ gradients between middepth Site 1088 and the deeper sites during glacial periods and subtle gradients during interglacial stages. The SPECMAP $\delta^{18}O$ record is shown for reference to oxygen isotope stages (modified after Hodell et al., in press a).

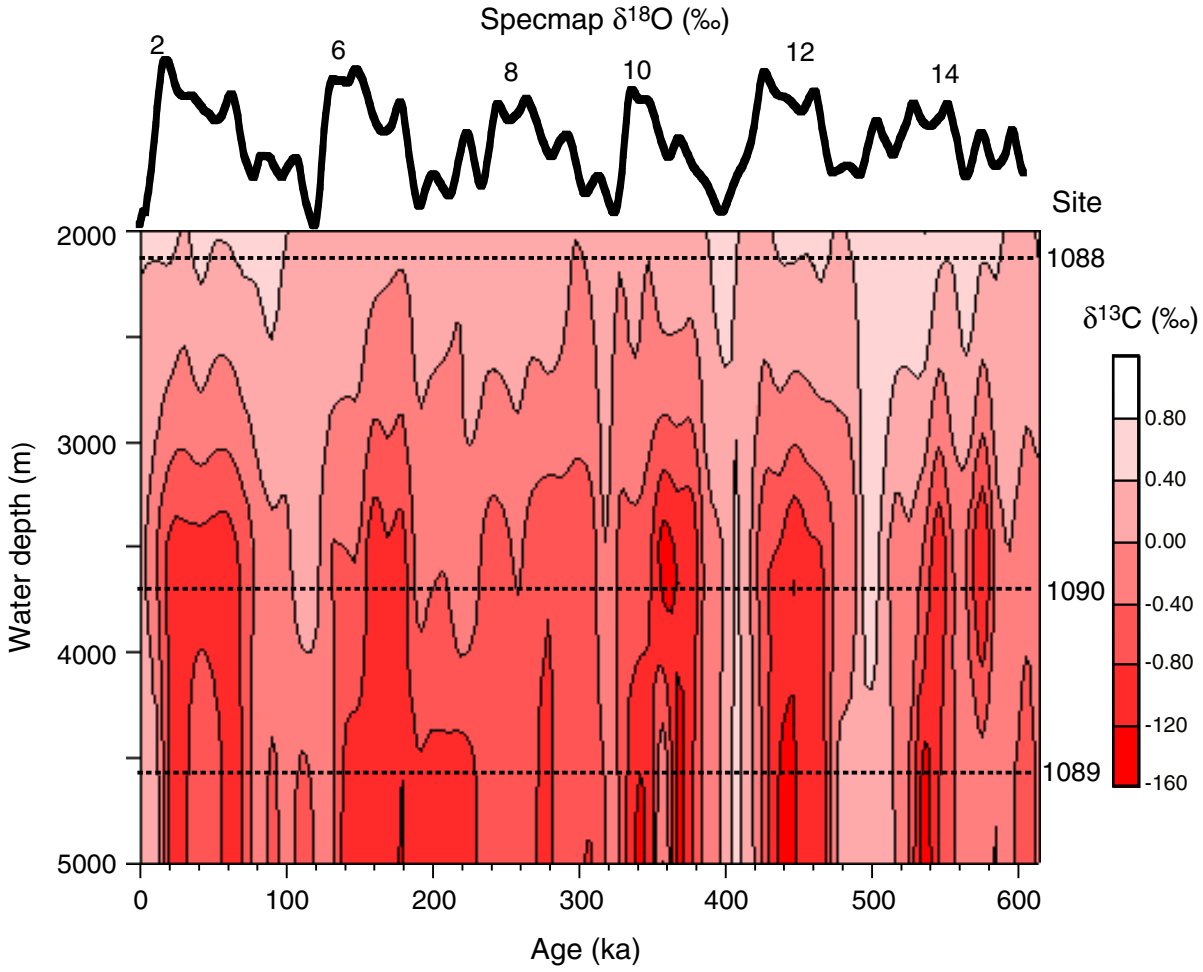

Figure F18. Reconstruction of vertical $\delta^{13}C$ gradients in the South Atlantic for the Holocene (blue line, solid circles) and last glacial maximum (red line, solid squares). Data were combined from Leg 177 sites with those of Mackensen et al. (2001) and Ninnemann and Charles (2002) (modified after Hodell et al., in press a).

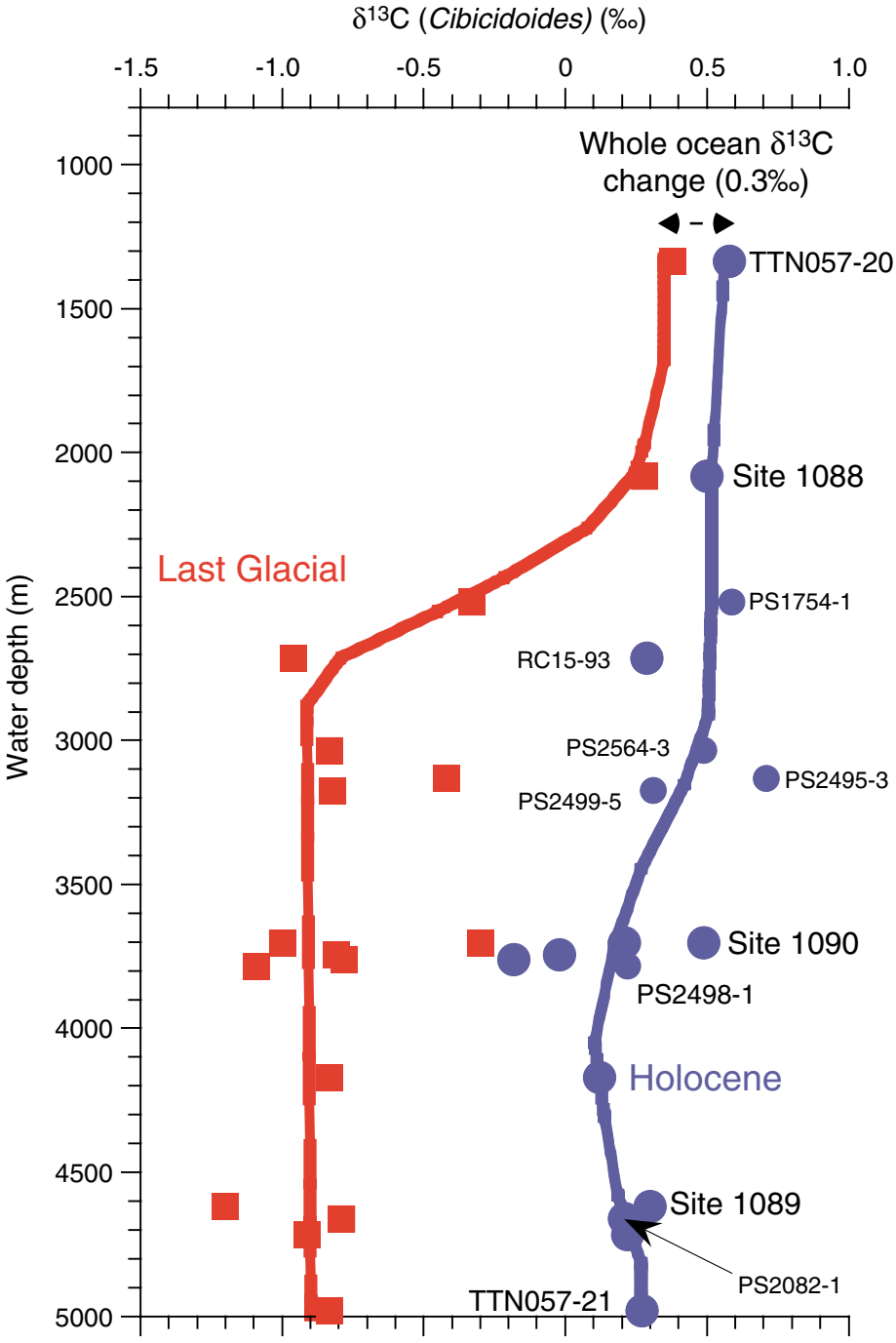

Figure F19. Changes in vertical carbon isotope gradients ($\delta^{13}C$) in the South Atlantic compared to pCO_2 variation in the Vostok ice core for the last 420 k.y. (Petit et al., 1999). $\Delta^{13}C$ represents the carbon isotopic gradient between middepth and deep waters, calculated by subtracting benthic $\delta^{13}C$ signals at Sites 1088 and 1090 after interpolating at constant 5-k.y. intervals (after Hodell et al., in press a).

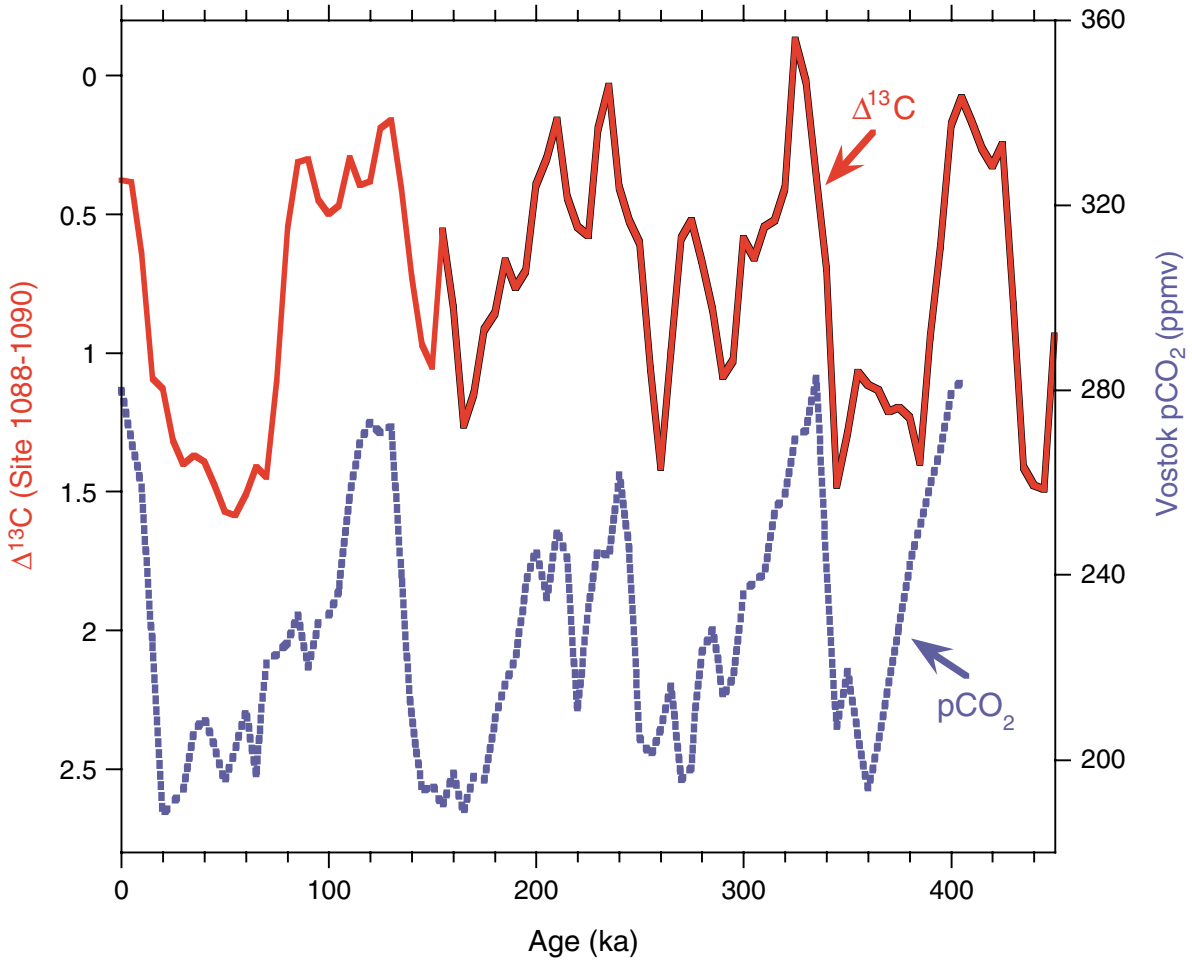

Figure F20. Evolutionary power spectra of selected sediment parameters from Site 1090. Kao = kaolinite, C = chlorite, Qz = quartz, Fsp = feldspar, orgC = organic carbon (after Diekmann and Kuhn, 2002).

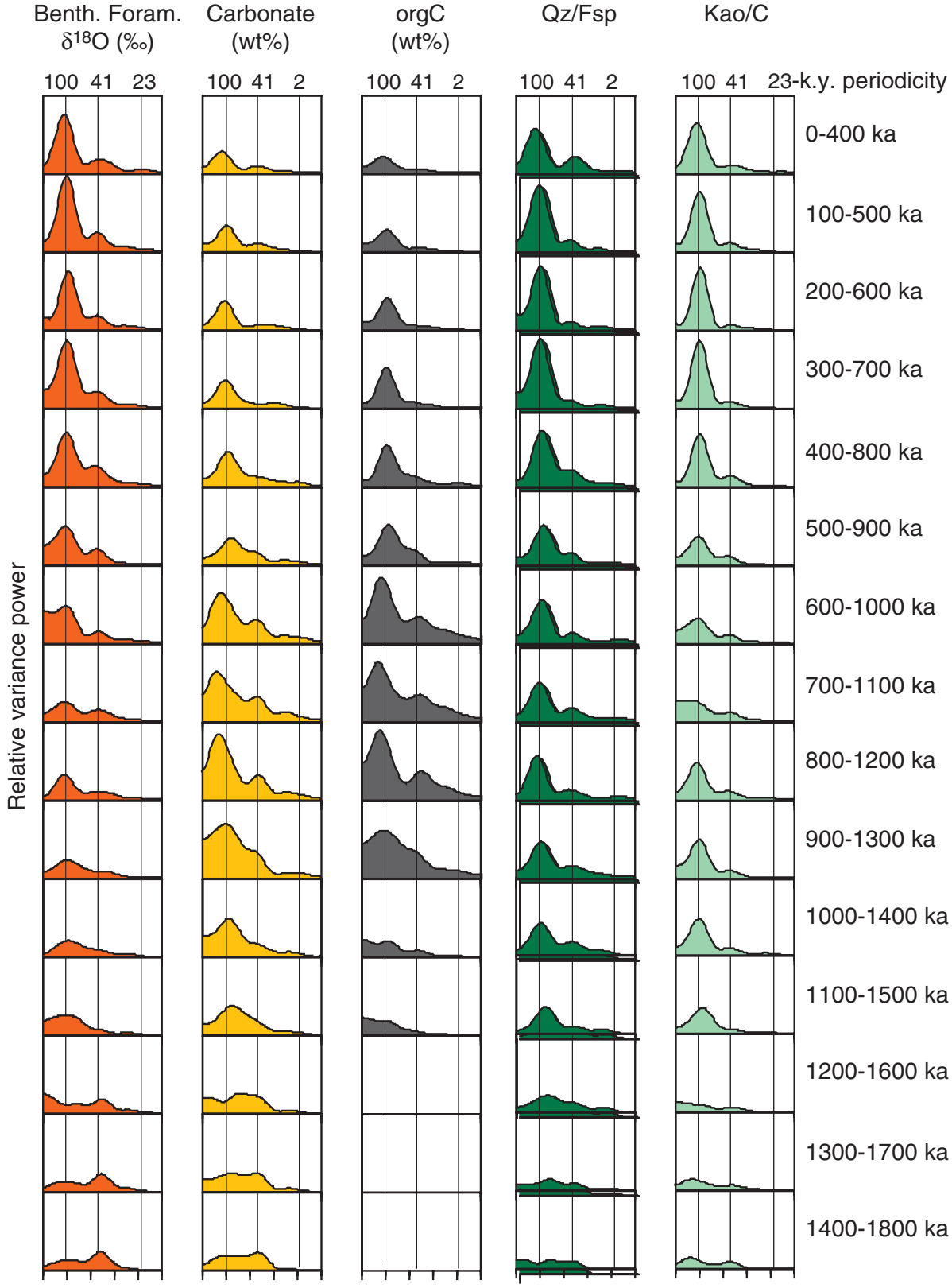

Figure F21. Carbonate (red line) and benthic $\delta^{18}O$ (black line) signals from Site 1089 showing the "Pacific-type" carbonate stratigraphy marked by high carbonate during glacials and low carbonate during interglacials. The benthic $\delta^{18}O$ signal leads the carbonate signal by an average of ~7.6 k.y. (after Hodell et al., 2001).

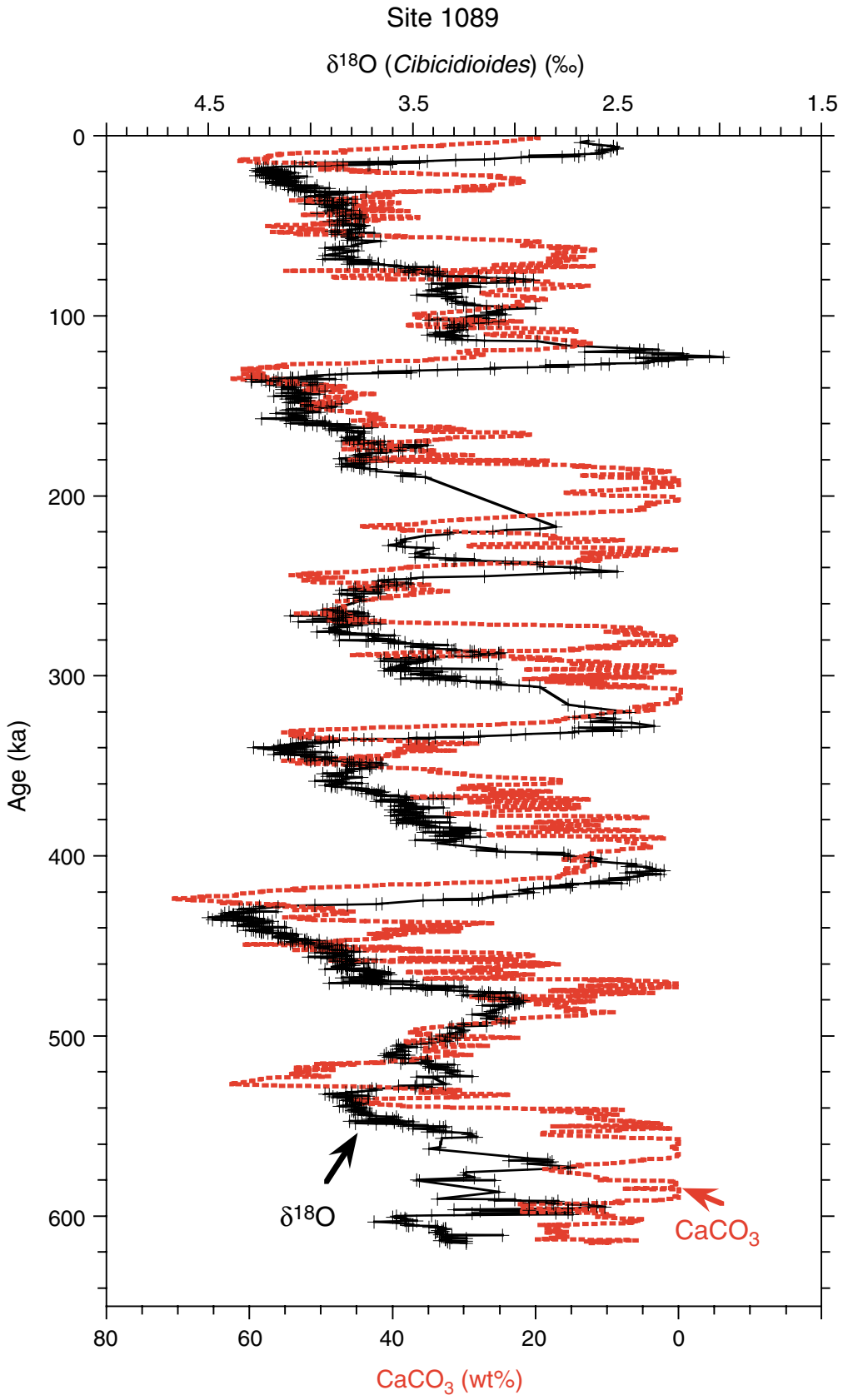

Figure F22. Comparison of the percent fragmentation of planktonic foraminifers (blue line) and weight percent carbonate (red line) at Site 1089 (Hodell et al., 2001) with the carbonate dissolution index (CDI) from the Indian Ocean (Peterson and Prell, 1985). The carbonate signal is very similar to Indo-Pacific dissolution records, but Site 1089 has greater fidelity because of its high sedimentation rates.

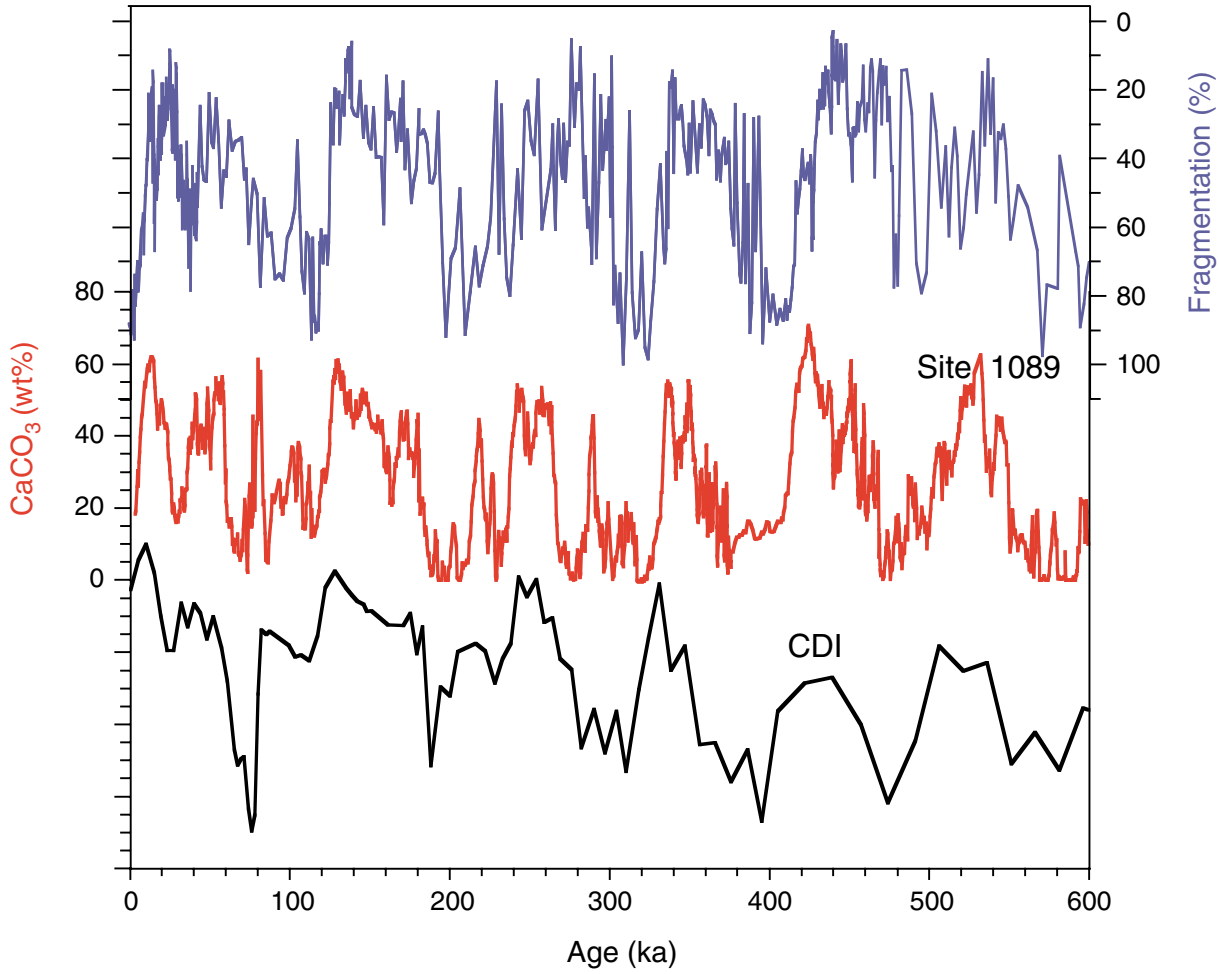

Figure F23. Correlation of the planktonic $\delta^{18}O$ signal at Site 1089 with Vostok δD. This correlation permits development of a marine chronology for the Vostok ice core and comparison of the relative phasing of atmospheric and oceanic variables (after Ninnemann et al., 1999 and Mortyn et al., submitted [N5]).

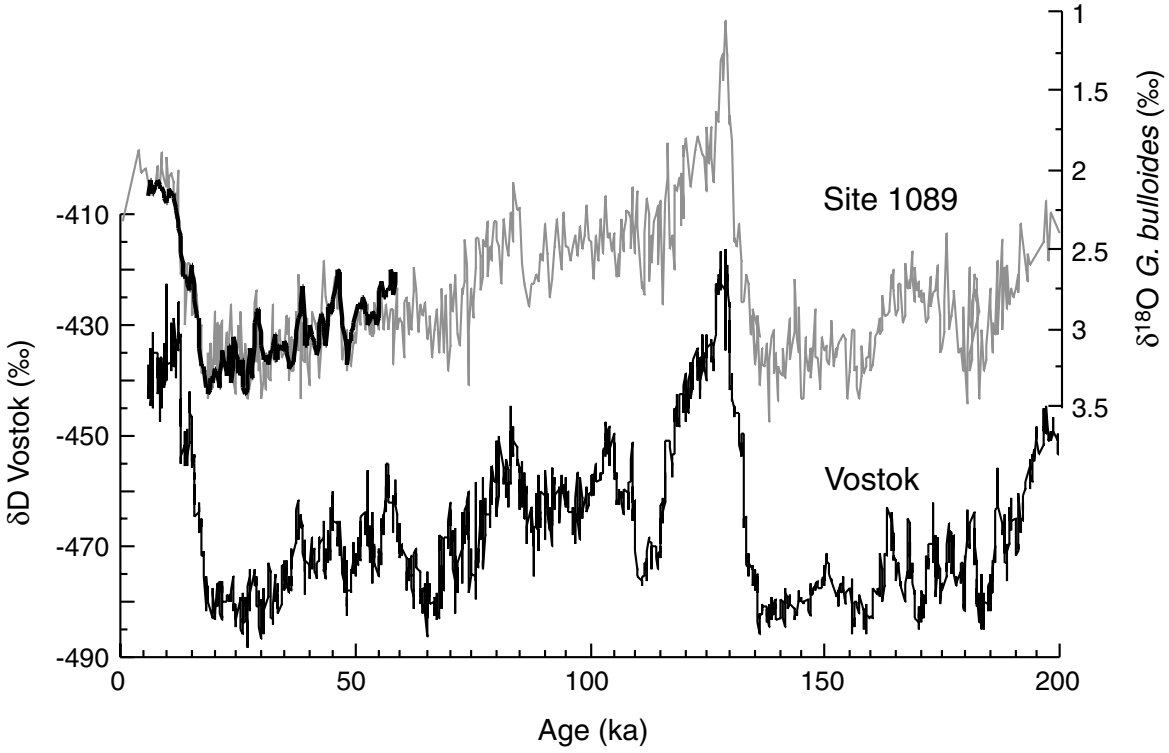

CHAPTER NOTES*

N1. Diekmann, B., Kuhn, G., Gersonde, R., Mackensen, A., submitted a. Middle Eocene to early Miocene climate development and reorganization of ocean circulation: evidence from biogenic and terrigenous depositional patterns in the Southern Ocean. *Global Planet. Change*.

N2. Censarek, B., and Gersonde, R., submitted. Middle to late Miocene climate evolution of the Southern Ocean derived from the diatom record at ODP sites 689, 690, 1088, and 1092. *Paleoceanography*.

N3. Diekmann, B., Fälker, M., Kuhn, G., submitted b. Environmental history of the southeastern South Atlantic since the middle Miocene. Evidence from the sedimentological records of ODP Sites 1088 and 1092. *Sedimentology*.

N4. Pearce R.B., Kemp, A.E.S., and Grigorov, I., submitted. Occurrence and distribution of laminated diatom mats (LDM) deposits in the Atlantic sector of the Southern Ocean, ODP Leg 177. *Palaeogeography, Palaeoclimatology, Palaeoecology*.

N5. Mortyn, P.G., Charles, C.D., Ninnemann, U.S., Ludwig, K., and Hodell, D.A., submitted. Deep sea sedimentary analogs for the Vostok ice core. *J. Geophys. Res*.

*Dates reflect file corrections or revisions.